

## Altered Fatty Acid Metabolism in Long Duration Road Transport: An NMR-based Metabonomics Study in Sheep

Juan Li,<sup>†,‡</sup> Gene Wijffels,<sup>\*,†</sup> Yihua Yu,<sup>‡</sup> Lars K. Nielsen,<sup>§</sup> Dominic O. Niemeyer,<sup>||</sup> Andrew D. Fisher,<sup>||,⊥</sup> Drewe M. Ferguson,<sup>||</sup> and Horst Joachim Schirra<sup>#</sup>

<sup>†</sup>CSIRO Livestock Industries, Queensland Bioscience Precinct, 306 Carmody Road, St Lucia, Queensland 4067, Australia

<sup>‡</sup>Shanghai Key Laboratory of Magnetic Resonance, Department of Physics, East China Normal University, 3663 North Zhongshan Road, Shanghai 200062, P.R. China

<sup>§</sup>Australian Institute for Bioengineering and Nanotechnology, The University of Queensland, Building 75, Cooper Road, Brisbane, Queensland 4072, Australia

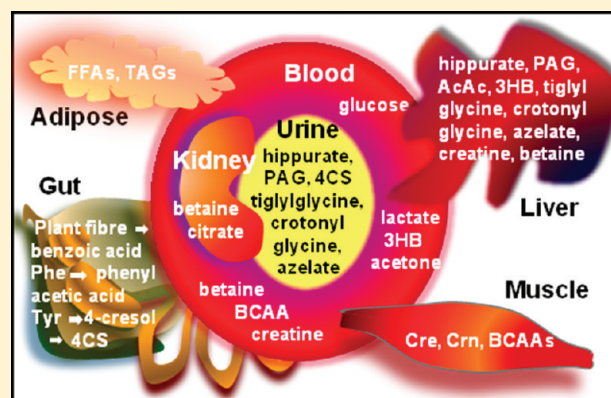
<sup>||</sup>CSIRO Livestock Industries, F.M. McMaster Laboratory, Locked Bag 1, Armidale, NSW 2350, Australia

<sup>#</sup>School of Chemistry and Molecular Biosciences, The University of Queensland, Building 76, Cooper Road, Brisbane, Queensland 4072, Australia

Supporting Information

**ABSTRACT:** The physical, endocrine, and metabolic responses of livestock to road transport have been evaluated by conventional hematological and biochemistry parameters for more than 20 years. However, these measures are relatively insensitive to subtle metabolic adaptations. We applied NMR-based metabonomics to assess system-wide metabolic responses as expressed in urine and serum of a large cohort of animals ( $n = 80$ ) subjected to 12 and 48 h road transport. The profiling of  $^1\text{H}$  NMR spectra revealed that the transported animals experienced altered gut and energy metabolism, muscle catabolism, and possibly a renal response. The animals transported for 48 h exhibited a deeper metabolic response to the transport event and a complex and expanded metabolic trajectory over the 72 h recovery period. Intriguingly, excretion of acyl glycines and a dicarboxylic acid was observed after transport and during recovery, implicating peroxisomal fatty acid oxidation as a metabolic response to transport-induced stress.

**KEYWORDS:** metabonomics, transport, stress, fasting, sheep, dicarboxylic acid, azelate, acyl glycine, crotonyl glycine, tiglylglycine



### INTRODUCTION

The application of metabonomic approaches to biological questions is rapidly expanding as its tools and methodologies are continually refined and become more accessible. As a field of study, it is described as “the quantitative measurement of the dynamic multiparametric metabolic response of living systems to pathophysiological stimuli or genetic modification”.<sup>1</sup> Metabonomics attempts to assess the whole metabolic profile in living biological systems and has the potential to become an important tool in unravelling the biochemical consequences of disease and describing altered physiological states induced by genetic mutations, drugs, diet, exercise and stress.<sup>2–6</sup> Two major approaches used in metabonomics to analyze the metabolic composition of samples include  $^1\text{H}$  nuclear magnetic resonance (NMR) spectroscopy and mass spectrometry (MS), in conjunction with chemometric techniques. In mammalian/vertebrate systems, NMR-based metabonomics has yet to be applied to many species outside humans and rodents, although there is now evidence of broader uptake through reports in livestock species such as salmon, cattle, sheep and pigs.<sup>7–13</sup>

NMR-based metabonomics has been particularly successful in describing subtle changes in the metabolic signatures in urine and plasma induced by acute and chronic physical and/or psychological stresses<sup>6,7,14–16</sup> as well as weight loss and fasting.<sup>17,18</sup> With this in mind, we have applied NMR-based metabonomics to an animal welfare and production issue: the long duration road transport of livestock. The metabolic and endocrine changes experienced by ruminants during and after transport are due to a combination of deprivation of food and water prior to and during transport and the stress response to the social and physical impacts of loading/unloading activities, transport conditions and duration.<sup>19–21</sup> The extent of metabolic change, time to recovery and interventions to improve recovery to avoid disruption of growth and immune status are of interest to the industries and their regulators.

Specifically, we conducted a global metabolic analysis using NMR-based metabonomics of both serum and urine from sheep

**Received:** August 24, 2010

**Published:** December 13, 2010

to assist in differentiating the metabolic responses and describing the recovery trajectories of two groups of sheep transported for 12 and 48 h under standard industry practices. A previous study on this same cohort of 40 mature animals per transport group showed no statistical differences between the metabolic responses to the two different treatments as determined by traditional hematological and clinical biochemistry assays,<sup>22</sup> thus providing the foundation as to whether a metabolomic study could implicate pathways not detectable by conventional approaches. Furthermore, with no access to food and water for the duration of the transport treatment, and with physical activity constrained, variability from these factors was much reduced.

We now report the systemic metabolic perturbation relative to pretransport conditions for each transport duration, and note the amplified impact of the 48 h transport duration. We map the recovery trajectory through the 72 h following arrival. We attempt to uncover the broader metabolic response to the perturbation, and nominate new possible indicator metabolites of severity of perturbation and recovery. We find that the ruminant metabolic profile was distinctly different in the appearance of a number of urinary products in both the 12 and 48 h transport groups on arrival and during recovery when drawing parallels with rodent and human models of under-nutrition or fasting. We suggest that ruminants may utilize the peroxisomal, and even microsomal, fatty acid oxidation systems to a greater extent than rodent and humans during metabolic stress.

## MATERIALS AND METHODS

### Animals

Urine and serum samples were collected during a road transportation experiment described by Fisher et al.<sup>22</sup> Briefly, 80 weight-matched Merino ewes of 4–5 years age were allocated to 4 road transport event groups each of 20 sheep. Two groups were subjected to 12 h road transportation and the other two groups subjected to 48 h transport duration. The two replicates for each treatment were conducted over a 13 day period (30th October to 11th November 2006). The transport events were arranged so that the treatments groups of each replicate experiment arrived at the same time on the same day to be simultaneously assessed and sampled. During the two replicate travel periods of 48 h duration, average daily maxima and minima temperatures were 21.8 and 21.2 °C and 9.3 and 9.9 °C, respectively. Cumulative rainfalls over the transport events were 0.8 and 8.8 mm. During the two 72 h recovery periods, average daily maxima temperatures and minima temperatures were 18.7 and 21.2 °C and 11.2 and 9.4 °C, respectively. The major weather difference between the two replicates was a total of 73 mm of rain experienced during the recovery period of the first replicate groups. The second replicate recovery period experienced 8.2 mm of rain. To reproduce industry practice, the 20 focal ewes of each group were loaded together with 350–450 other sheep onto commercial sheep transport semitrailers fitted with identical stockcrates. Prior to transport, the animals were grazed good quality spring pasture. After transport, the sheep were unloaded into sheep yards and given *ad libitum* food (high quality hay) and water. Blood and urine samples were taken from the 20 focal animals at the time of loading onto the vehicles (pre-transport), at arrival (0 h), and through the recovery period at 24, 48 and 72 h post-transport (Figure 1). Blood was collected by venepuncture of the jugular vein and the flow directed into an EDTA treated serum separator vacuum tubes (BD).<sup>22</sup> After centrifugation (2800 × g, 15 min, 4 °C), the serum was removed

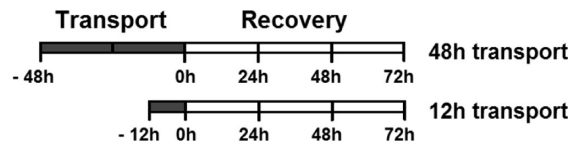


**Figure 1.** Experimental design of the sheep road transport experiment. Two replicate experiments were conducted. Each experiment subjected one group of 20 sheep to 12 h transport and a second group of 20 sheep to 48 h transport. In each replicate experiment, the 12 and 48 h transport groups arrived at the same time on the same day. Urine and sera were collected at the indicated time points: pretransport, arrival and during recovery.

and stored (−20 °C) until required. Urine was sampled via an urethral catheter attached to a syringe.<sup>22</sup> The withdrawn volume (3–4 mL) was placed into a sterile container, and then stored at −20 °C. Five urine samples from various time points could not be collected due to emptied bladders (see Supplementary Table S1, Supporting Information). All samples had been stored for 2 years (−20 °C) at the time of these studies.

Examination of the clinical biochemical data collected by Fisher et al. (2010) reveals that there were no differences in the replicates for each transport event over the time course in regard to live weight, urine specific gravity, plasma cortisol and serum albumin. Differences (greater than one standard deviation) were observed between the 12 h transport replicates in respect to plasma creatine kinase at pretransport and serum urea and serum total protein on arrival. The two 48 h transport replicates exhibited greater than one standard deviation difference in serum 3-hydroxybutyrate at 24 h recovery only (data not shown).

The data was also examined for outliers that may influence analyses of replicate responses. We defined an outlier as returning measures equal to or greater than three standard deviations of the mean of all the measures for the relevant parameter. No individual animal was a consistent outlier over the course of the transport experiments for the clinical biochemical data and live weight assessments conducted by Fisher et al. (2010). Only 4 individual animals returned results greater than three standard deviations for 2 or 3 of these parameters and only at single time points. On these bases, no animal was clearly ill or responding differently relative to the other members of the group. Due to low frequency of these outlier events, these animals were not removed from the metabolomic analyses.

### <sup>1</sup>H NMR Spectroscopy of Serum and Urine Samples

Serum and urine samples were thawed at RT for sample preparation. A 200 μL aliquot of each serum sample was diluted with 400 μL 0.9% w/v NaCl containing 10% D<sub>2</sub>O as a field frequency lock. A 400 μL aliquot of each urine sample was mixed with 150 μL 1 M sodium phosphate buffer (pH 7.4) and 50 μL D<sub>2</sub>O. Precipitates were removed from the diluted serum and urine samples by centrifugation (12 000 × g) for 5 and 10 min, respectively. An internal chemical shift standard 2,2-dimethyl-2-sila-3,3,4,4,5,5-hexadeuteropentane-5-sulfonic acid (DSS), and an internal pH indicator, 1,1-difluoro-1-trimethylsilyl methyl phosphonic acid dissolved in D<sub>2</sub>O, were added to 540 μL of the diluted urine sample to give final concentrations of 18.2 μM each and a final sample volume of 550 μL. The prepared samples (550 μL) were transferred into 5 mm NMR tubes. <sup>1</sup>H NMR spectra were acquired at 298 K on a Bruker AV500 NMR spectrometer operating at a <sup>1</sup>H frequency of 500.13 MHz, equipped with a 5 mm self-shielded z-gradient triple resonance probe, and a B-ACS 60 sample changer.

Two types of  $^1\text{H}$  NMR spectra were acquired for serum samples: (a) 1D NOESY spectra were acquired with the standard noesypr1d pulse sequence [(RD)- $90^\circ$ - $t_1$ - $90^\circ$ - $\tau_m$ - $90^\circ$ -acq] (Bruker Biospin pulse program library). The water signal was suppressed by continuous wave irradiation during both the relaxation delay of 2.3 s, and the mixing time ( $\tau_m$ ) of 100 ms. (b) Water-suppressed Carr-Purcell-Meibom-Gill spectra were acquired with the cpmgpr1d pulse sequence [RD- $90^\circ$ -( $\tau$ - $180^\circ$ - $\tau$ )<sub>n</sub>-acq] (Bruker Biospin pulse program library). A fixed spin-spin relaxation delay  $2n\tau$  of 20 ms ( $\tau = 500 \mu\text{s}$ ) was used to eliminate the broad signals from high molecular weight analytes, and water suppression irradiation was applied during the relaxation delay of 2.3 s. For both types of spectra, 32,768 data points with a spectral width of 14.0 ppm were collected into 256 transients and 16 dummy scans. Similar 1D NOESY experiments as described above were carried out on urine samples.

All spectra were processed using TOPSPIN version 1.3 (Bruker Biospin, Rheinstetten, Germany). The free induction decays were multiplied by an exponential window function corresponding to 0.3 Hz line broadening factor before Fourier Transformation. The acquired spectra were manually phased and baseline-corrected. The spectra of serum samples were referenced to lactate ( $\text{CH}_3$ ,  $\delta = 1.33 \text{ ppm}$ ) and the urine spectra were referenced against DSS.

Spectra from 394 urine samples and 396 serum samples were included in this study. Five urine samples were not able to be collected, and one sample yielded bad quality spectra. Four serum samples were unavailable for NMR analysis due to their consumption in prior assays.<sup>22</sup> A minimum of 19 sera (of an original set of 20) were measured for each group and time point, and a minimum of 18 (out of 20) urine samples were measured for each group and time point (Supplementary Table S1, Supporting Information). The samples had been stored at  $-20^\circ\text{C}$  for 2 years at the time of these studies. While the possibility of sample degradation during prolonged storage can in principle not be excluded, any degradation process would incur a systemic effect on all samples rather than a selective effect on any group of samples. Levels of formate, ethanol and acetate in urine remained constant during the analysis of these samples which is evidence that bacterial activity was not detectable, thus the stability of samples is considered reliable.

The assignment of metabolites was based on literature data<sup>23,24</sup> and the online metabolomics databases, Human Metabolome Database (<http://www.hmdb.ca/>) and Biological Magnetic Resonance Bank (<http://www.bmrb.wisc.edu/metabolomics>). Assignments were confirmed by 2-dimensional (2D)  $^1\text{H}$ - $^1\text{H}$  double-quantum filtered correlation spectroscopy (DQF-COSY),<sup>25</sup>  $^1\text{H}$ - $^1\text{H}$  total correlation spectroscopy (TOCSY),<sup>26</sup>  $^1\text{H}$ - $^{13}\text{C}$  heteronuclear single quantum coherence (HSQC)<sup>27,28</sup> and  $^1\text{H}$ - $^{13}\text{C}$  heteronuclear multiple bond correlation (HMBC)<sup>29</sup> spectra measured on selected samples. The 2D NMR spectra were acquired on a Bruker Avance 900 spectrometer operating at a  $^1\text{H}$  frequency of 900.13 MHz, equipped with a 5 mm self-shielded z-gradient triple resonance cryogenic probe. In all 2D spectra, the  $^1\text{H}$  carrier frequency was positioned on the water resonance. Homonuclear 2D spectra were acquired with a spectral width of 12.0 ppm in both dimensions. 512 increments with 32 transients were recorded in the time-proportional phase incrementation (TPPI) mode,<sup>30</sup> requiring a total acquisition time of 6.5 h. The relaxation delay was set to 1 s. TOCSY experiments used a MLEV-17 spin-lock scheme<sup>31</sup> of 80 ms duration for isotropic mixing. Prior to Fourier transformation, the resulting NMR spectra were zero filled to 1024 points in the indirect dimension and multiplied by a squared sine

bell window function shifted by  $\pi/2$  in the indirect dimension, while a Lorentz to Gauss transformation with a line broadening factor of  $-10 \text{ Hz}$  and a Gaussian broadening factor of 0.1 was applied in the direct dimension.

HSQC and HMBC experiments were performed with spectral widths of 12 ppm and 200 ppm in the  $^1\text{H}$  and  $^{13}\text{C}$  dimensions, respectively. 512 increments (each 4096 data points) with 64 and 16 transients, respectively, were recorded, and a relaxation delay of 1.0 s was used. HSQC experiments were recorded in echo-antiecho mode, while the QF mode was used in HMBC experiments. The spectra were multiplied by a squared sine bell window function shifted by  $\pi/2$  along the direct and indirect dimensions before two-dimensional Fourier transformation.

### Data Reduction

The 1D  $^1\text{H}$  NMR spectra of serum samples were automatically data-reduced to consecutive integral regions of equal width of 0.02 ppm ("buckets") covering the range of  $\delta = 0.3\text{--}10 \text{ ppm}$  using the software AMIX (Analysis of Mixtures software package, version 3.6.6, Bruker Biospin). To eliminate the effects of imperfect water suppression, cross-saturation of urea, and the disproportionate influence of dominating peaks from lactate on normalization,<sup>32</sup> the chemical shift regions at  $\delta 4.68\text{--}6.0 \text{ ppm}$ ,  $\delta 4.10\text{--}4.18 \text{ ppm}$  and  $\delta 1.32\text{--}1.36 \text{ ppm}$ , were excluded from serum spectra. The spectra of urine samples were data reduced in a similar fashion, using the chemical shift range of  $\delta = 0.2\text{--}10 \text{ ppm}$  in the analysis and excluding the region  $\delta 4.5\text{--}6 \text{ ppm}$ . For each spectrum, the data were normalized to the total intensity of the spectrum. The resulting bucketed data matrices were imported into the SIMCA-P+ 12.0 software package (Umetrics AB, Sweden) for multivariate statistical analysis (MVSA).

### Multivariate Statistical Analysis

The sheep urine spectra were scaled by pareto scaling, to minimize the effect of dynamic range of signal intensity of urinary metabolites. In serum spectra, the sharp peaks from small molecules were overlapped with broad signals from macromolecules, which potentially reduced their original intensity. To avoid over-emphasizing the baseline noise regions of the NMR spectra or small signals whose variation is dominated by baseline noise, center-scaled data were used in MVSA of serum.

Principle components analysis (PCA) was performed on both urine and serum samples to investigate inherent differences in the samples. Separation among samples from different time points of the 12 and 48 h transport duration groups was observed (data not shown). In the PCA analysis a few pretransport or arrival samples (15 serum samples and 12 urine samples) could potentially be considered outliers according to the 95% Hotelling's T2 confidence range. However, all outliers are part of a continuous distribution of samples and come from the same replicates. These samples stray most likely beyond the 95% confidence level because of slight differences in the response between replicates. Batch modeling showed no individual animal consistently beyond three standard deviations over the time course. Thus, no samples were removed as outliers from the MVSA models.

To maximize the distinction between time points, partial least-squares-discriminant analysis (PLS-DA) was employed to analyze data. The class membership of individual sample was provided in form of a Y-table, against which the PLS algorithm performs a regression with the multivariate data. In our study, the group identity of pretransport, arrival and the 24 h, 48 h, 72 h recovery (post-transport) samples of the 48 and 12 h transport groups were used as the Y-table. In SIMCA, the number of PLS

**Table 1. Properties of PLS-DA Models of Urine and Serum Samples<sup>a</sup>**

model	sample	transport duration/time points	scaling	N	nPLS	R <sup>2</sup> X	R <sup>2</sup> Y	Q <sup>2</sup>
M1	Urine	48 h/all	Pareto	195	8	82.70%	73.10%	61.70%
M2	Urine	12 h/all	Pareto	199	8	77.40%	61.10%	44.60%
M3	Serum	48 h/all	Centered	197	11	88.60%	64.10%	47.10%
M4	Serum	12 h/all	Centered	199	7	80.50%	51.00%	39.40%
M5	Urine	12 h + 48 h/Pre + Arr	Pareto	157	7	80.90%	85.50%	78.50%
M6	Serum	12 h + 48 h/Pre + Arr	Centered	160	7	82.80%	71.90%	62.10%
M7	Urine	48 h + 12 h/all	Pareto	394	13	85.50%	62.60%	49.80%
M8	Serum	48 h + 12 h/all	Centered	396	12	88.00%	54.40%	43.10%

<sup>a</sup> N, number of spectra in the model; nPLS, number of PLS components; Pre, pre-transport; Arr, arrival.

components for the model was optimized by cross validation. R<sup>2</sup>X, R<sup>2</sup>Y and Q<sup>2</sup> were used to evaluate model quality. R<sup>2</sup>X and R<sup>2</sup>Y, which are the fraction of the sum of squares for the selected component, represent the variance of X and Y variables, and Q<sup>2</sup> is the predictive ability parameter of the model which is estimated by the default leave 1/7 out cross validation. The corresponding values for the eight PLS-DA models are displayed in Table 1. Permutation tests were performed 200 times to validate PLS-DA models (Supplementary Figure 2, Supporting Information). Scores plots and Loadings plots combined with variable importance in the projection (VIP) were used to interpret the various PLS-DA models. O2PLS analyses were performed on urine and serum spectra from sheep transported for 12 and 48 h, respectively, to examine the correlation between urinary and serum metabolites.

### Univariate Statistical Analysis

Metabolites observed to change significantly in the multivariate analysis were each explored further using univariate analysis. The increment seen during transport and the trend seen during recovery were analyzed separately. Analyses were performed in R using the lme4 package for the mixed effect models.

**Increment.** Increments during transport were first analyzed using 2-way ANOVA to assess if there was an effect of transport and if there was block and/or interaction effects between the replicate experiments.

If there were no significant block and/or interaction effects, the data were fitted to the linear model

$$\begin{aligned} \text{Increment}_{n(ij)} &= M_{n(ij)}^{\text{Arrival}} - M_{n(ij)}^{\text{Pretransport}} \\ &= \text{treatment}_i + \text{Error}_{n(ij)} \end{aligned}$$

where n is the animal number, i = {12 h, 48 h} is the transport time, and j = {A, B} is the experimental block. The significance of the two contrasts – ( $\mu_{12\text{ h}} - 0$ ) and ( $\mu_{48\text{ h}} - \mu_{12\text{ h}}$ ) – were used, respectively, to assess whether 12 h transport had a significant effect and if extended 48 h transport had a further effect.

If a significant block and/or interaction effect was observed, the four treatment:block effects were estimated using the linear model

$$\begin{aligned} \text{Increment}_{n(ij)} &= M_{n(ij)}^{\text{Arrival}} - M_{n(ij)}^{\text{Pretransport}} \\ &= (\text{treatment : block})_{ij} + \text{Error}_{n(ij)} \end{aligned}$$

The same contrasts as above were used to assess significance, except here applied and reported separately for the A and B block.

**Trend.** The trend during recovery was fitted using a linear mixed effect model allowing for random variations in parameters

between animals. First, four individual models were fitted for each treatment and block combination:

$$\begin{aligned} M_{ijkn} &= \text{intercept}_{ij} + I_{n(ij)} + (\text{trend}_{ij} + T_{n(ij)}) \\ &\quad \times \text{time}_k + \text{Error}_{n(ijk)} \end{aligned}$$

where n is the animal number, i = {12 h, 48 h}, j = {A, B}, and time = {0 d, 1 d, 2 d, 3 d}. I and T are the random animal contributions to intercept and trend, respectively.

The model was reduced in two steps

$$\begin{aligned} M_{ijkn} &= \text{intercept}_i + I_{n(i)} + (\text{trend}_i + T_{n(i)}) \\ &\quad \times \text{time}_k + \text{Error}_{n(ijk)} \text{ [No block effect]} \end{aligned}$$

$$\begin{aligned} M_{ijkn} &= \text{intercept} + I_n + (\text{trend} + T_n) \\ &\quad \times \text{time}_k + \text{Error}_{n(ijk)} \text{ [No treatment effect]} \end{aligned}$$

The models were compared using a likelihood ratio test and, where not significant, the reduced model was chosen.

## RESULTS

We determined the metabolic profiles of sheep during road transport by measuring one-dimensional <sup>1</sup>H NMR spectra of urine and serum samples. Typical spectra with assignments of some metabolites are shown in Figure 2. Visual inspection of these spectra revealed subtle variation between different time points for both types of samples. As the NMR spectra were too complex for objective visual analysis, MVSA was used to analyze the metabolic differences between samples in detail. To maximize the distinction between time points, supervised MVSA (PLS-DA) was performed, confirming findings from explorative PCA (data not shown).

### PLS-DA Analysis of Urine Samples

PLS-DA produces two sets of figures: scores plots and loadings plots. Scores plots indicate how similar the metabolic profiles of the samples are to each other. Each data point represents one NMR spectrum (sample); in the scores plots, the clustering of data points indicates that the samples they represent have more similar metabolite composition, and vice versa. The loadings plots illustrate the metabolites responsible for the variation within the samples observed in the respective position in the corresponding scores plots. For urine samples, two PLS-DA models (Table 1, M1 and M2) of eight PLS components were calculated for the two transport durations, as shown in Figure 3 (only the first three components are shown). The time effect of the transport and subsequent 72 h recovery period was illustrated by the clustering of the samples from each time point in the scores plots (Figure 3A and B). Pretransport and arrival samples were neatly

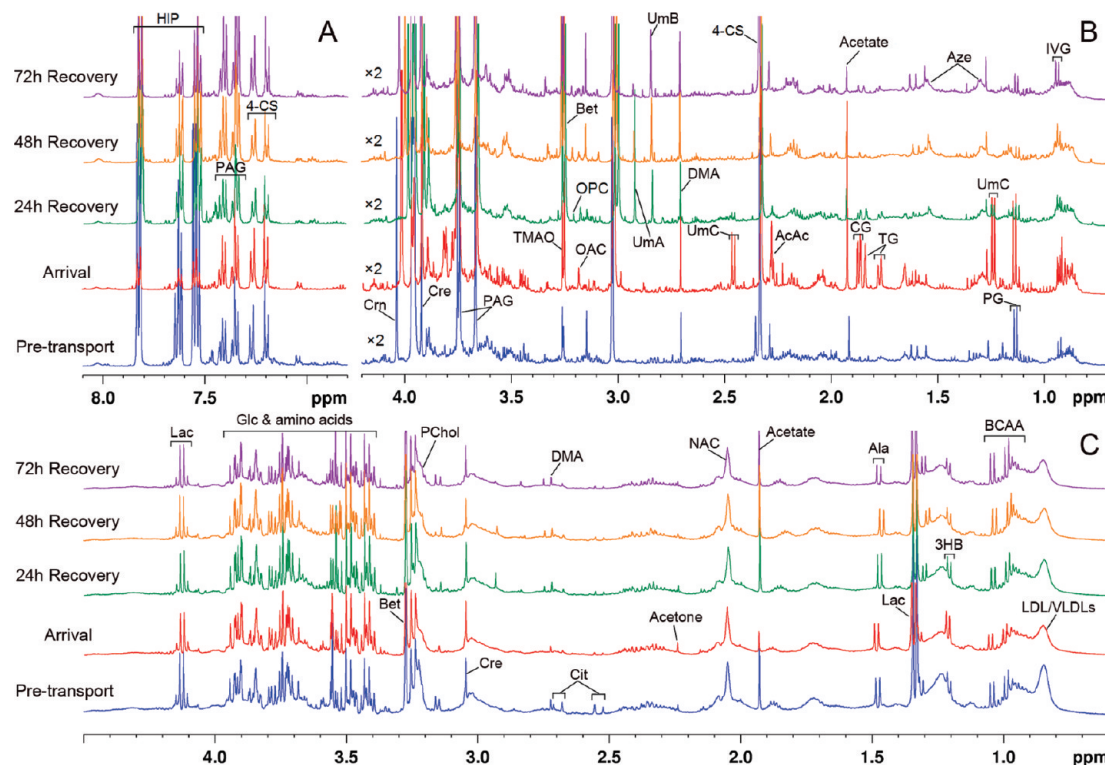


**Figure 2.** Typical NMR spectra of urine and sera samples from two different animals subjected to 48 h road transport. (A and B)  $^1\text{H}$  NMR 1D-NOESY spectra of the urine samples of a single animal at pretransport (blue), arrival (red), and 24 h (green), 48 h (gold) and 72 h (purple) recovery. (C)  $^1\text{H}$  NMR 1D-CPMG spectra of the sera of a single animal sampled at pretransport, arrival, and 24 h, 48 and 72 h recovery (using the same color regime as A and B). Various metabolites are assigned: 3HB, 3-hydroxybutyrate; 4-CS, 4-cresol sulfate; AcAc, acetoacetate; Ala, alanine; Aze, azelate; BCAA, branched-chain amino acids; Bet, betaine; Cit, citrate; Cre, creatine; Crn, creatinine; CG, crotonyl glycine; DMA, dimethylamine; Glc, glucose; HIP, hippurate; IVG, N-isovalerylglycine; Lac, lactate; LDL/VLDLs, low/very low density lipoproteins; NAC, N-acetyl glycoproteins; OAC, O-acetylcarnitine; OPC, O-phosphocholine; PAG, phenylacetylglycine; PChol, phosphatidylcholine; PG, propane 1,2-diol; TG, tiglylglycine; TMAO, trimethylamine N-oxide; UmA/B/C, unidentified metabolite A/B/C.

separated in both the first and second components ( $t_1$  and  $t_2$ ) of PLS-DA, which demonstrated that the metabolic profiles of sheep were perturbed during the transport process. During the recovery period, the metabolic profiles differed from those of the pretransport and arrival samples. The profiles of the 24 h post-transport samples were most distant from the previous two time points; however, the metabolic profiles of the later 48 and 72 h post-transport urines showed convergence to a new metabolic state. Furthermore, as the metabolic profiles of animals changed gradually in the recovery period, there was overlap between 24, 48 and 72 h recovery samples in the second and third components ( $t_2$  and  $t_3$ ) of PLS-DA (Figure 3A and B).

To focus solely on the perturbations induced by transport, a 7-component PLS-DA model was calculated using only the pretransport and arrival samples from both transport durations (Table 1, MS). The resulting model showed that the pretransport samples of both transport durations are similar to each other and separated from the arrival samples in the first component ( $t_1$ ), while the separation of the two arrival groups was in the first and second components (Figure 4A,  $t_1$  and  $t_2$ ). The profiles of the 48 h arrival samples were clearly different to the corresponding arrival samples of the 12 h transport group (Figure 4B).

To analyze the intrinsic variation of the urine metabolites between time points, the loadings plots were investigated. We found the levels of some metabolites changed over time. However, the statistical significance of these changes was difficult to determine using loading plots alone. This problem was overcome

in two different ways: First, we used Variable Importance in the Projection (VIP) to select relevant variables/metabolites. In PLS, the influence on Y of each variable in the model is termed VIP. Variables with VIP values  $>1$ , are considered as the most relevant for explaining  $\text{Y}^{33}$  and these variables/metabolites were selected for further analysis (Table 2). Second, we investigate the time course trajectory of individual compounds by calculating changes of relative concentrations (scaled by the total sum intensity of spectra) of the selected variables and analyzing their time development in a univariate fashion with a linear model using the lme4 library in the program package R. The data are presented in Table 3 and Supplementary Figure S1, Supporting Information. This linear modeling analysis allowed us not only to investigate the effect of transport duration (12 h versus 48 h), but also the block effect, that is, potential differences between the two replicate groups.

The linear modeling analysis (Table 3) indicates that most of the key metabolites that behave slightly differently between the two replicates occur during the transport phase, while only urinary citrate, lactate, O-acetylcarnitine, betaine, unidentified metabolite A (UmA) and serum creatine show replicate effects during the recovery phase. Therefore, replicate effects are mainly found at pretransport and arrival. These results have also been confirmed by investigating replicate effects in the MVSA of urine samples (data not shown). Results showed the two 12 h replicates exhibited some difference in O-acetylcarnitine, betaine, UmA, and UmC at pretransport and arrival. The two 48 h replicates showed some differences

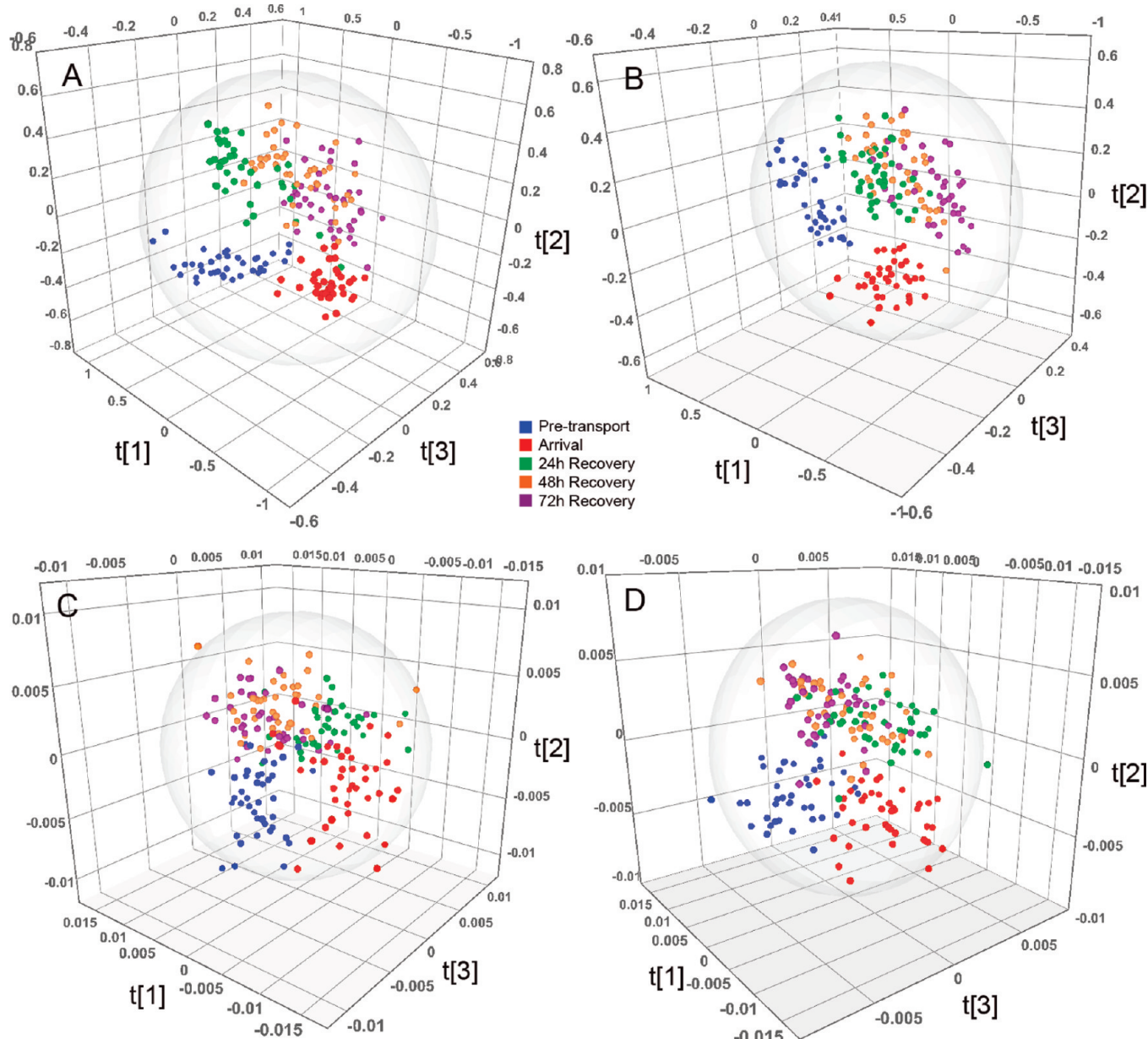


**Figure 3.** Partial least-squares-discriminant analysis (PLS-DA) of urine and serum metabolic profiles during road transport. (A and B) Scores plots of the first three PLS components arising from the urine samples of the animals transported for 48 h ( $R^2X [1] = 0.423$ ,  $R^2X [2] = 0.172$ ,  $R^2X [3] = 0.084$ ,  $R^2Y = 0.553$ ,  $Q^2 = 0.541$ ) and 12 h ( $R^2X [1] = 0.376$ ,  $R^2X [2] = 0.175$ ,  $R^2X [3] = 0.060$ ,  $R^2Y = 0.459$ ,  $Q^2 = 0.435$ ), respectively. (C and D) Scores plots of the first three PLS components arising from the serum samples of the animals transported for 48 h ( $R^2X [1] = 0.334$ ,  $R^2X [2] = 0.149$ ,  $R^2X [3] = 0.130$ ,  $R^2Y = 0.354$ ,  $Q^2 = 0.333$ ) and 12 h ( $R^2X [1] = 0.400$ ,  $R^2X [2] = 0.131$ ,  $R^2X [3] = 0.101$ ,  $R^2Y = 0.369$ ,  $Q^2 = 0.344$ ), respectively.

in hippurate, creatine and creatinine at pretransport and betaine at 0 h (arrival) and 24 h recovery. In serum, the differences in betaine and glucose at pretransport and lipoproteins and betaine on arrival can be observed in 48 h transport replicates. The two 12 h replicates showed no difference in the response. Thus, the MVSA results indicate the major replicate differences are at pretransport. The replicate differences in the responses to transport and recovery events are small and negligible compared to the transport/recovery responses themselves. To focus on the general metabolic responses to the two events, replicate effects will thus not be further discussed in this paper.

Both transport events were correlated with a decreased level of hippurate and increased levels of creatine, creatinine, phenylacetylethylglycine, 4-cresol sulfate, crotonyl glycine, tiglylglycine, betaine,

O-acetylcarnitine, and lactate. Analysis of 12 h transport duration arrival samples revealed that levels of acetoacetate and O-phosphocholine were also increased but decreased again within 24 h. However, acetoacetate and O-phosphocholine were not discriminating features in any of the 48 h transport samples ( $VIP < 1$ ), while the significantly increased levels of propane 1,2-diol only appeared in the recovery samples of 48 h transport groups. Hippurate decreased by 60% after 12 h transport, and a decrease of 90% was observed after 48 h transport (Table 3). Differences between the two transport durations were due to changes to creatine, creatinine, crotonyl glycine, tiglylglycine and betaine levels. Figure 4A and B revealed that arrival samples from 48 h transport groups had higher levels of creatine, creatinine, crotonyl glycine,

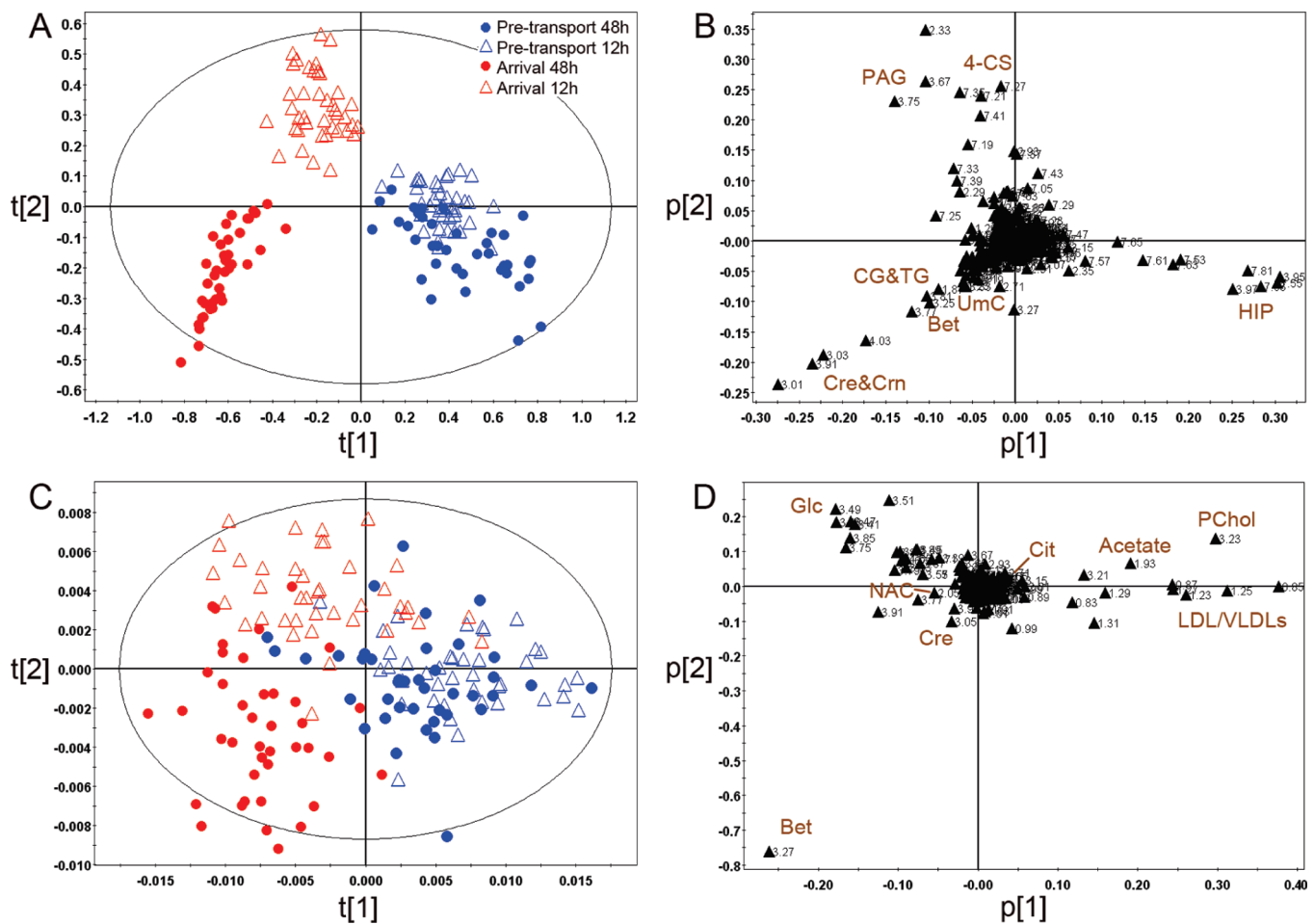


**Figure 4.** Comparison of pretransport and arrival metabolic profiles. (A and B) PLS-DA scores plot and corresponding loadings plot of pretransport (blue) and arrival (red) urines of 12 (open triangle) and 48 h (dot) transported groups ( $R^2X[1] = 0.512$ ,  $R^2X[2] = 0.135$ ,  $R^2Y = 0.568$ ,  $Q^2 = 0.564$ ). (C and D) PLS-DA scores plot and corresponding loadings plot of pretransport and arrival sera of the animals transported for 12 and 48 h ( $R^2X[1] = 0.472$ ,  $R^2X[2] = 0.122$ ,  $R^2Y = 0.379$ ,  $Q^2 = 0.363$ ). See Figure 2 legend for metabolite abbreviations.

tiglylglycine, betaine and UmC (d 1.24 ppm, d 2.46 ppm and q 4.22 ppm) compared with the arrival samples after 12 h transport. Therefore, the amplified effects of the longer transport duration on metabolic profiles were positively correlated with the increase of creatine, creatinine, crotonyl glycine, tiglylglycine, betaine and UmC and the decrease of hippurate. Betaine and UmA (s 2.93 ppm) increased to peak levels at 24 h recovery and decreased thereafter. Levels of azelate, O-acetyl carnitine, lactate, N-isovalerylglycine, UmB (s 2.85 ppm) and fatty acids remained elevated during the recovery.

An overall metabolic model of the perturbation induced by the transport events and subsequent recovery was derived by computing a combined PLS-DA model (Table 1, M7) containing the samples from both transport durations. The respective trajectories of the metabolic profiles caused by both transport treatments were calculated from the 3D scores plot of the model (Figure 5A). The amplified effect of the longer duration transport is clearly illustrated by the expanded trajectory experienced by the animals transported for 48 h, compared to the compressed trajectory developed by the animals transported for 12 h. In both cases, the largest changes occurred first between pretransport and arrival, and second between arrival and 24 h recovery. In the 12 h transport group, the later recovery time points were highly overlapped, in contrast to the corresponding time points of the

48 h transport group. It was apparent in both cases, that the end point state, despite 72 h recovery, was not equivalent to the pretransport state.

#### PLS-DA Analysis of Serum Samples

Two PLS-DA models were calculated for the sera from all five time points of 48 and 12 h transport groups (Table 1, M3 and M4). Pretransport and arrival samples were separated in the first PLS-DA component ( $t_1$ ) in the scores plots (Figure 3C and D), while the separation between recovery samples and the other samples was mainly contained in the second component ( $t_2$ ). Compared with the 12 h transport group, the clusters of pretransport and arrival samples of the 48 h transport group were more disperse, indicating larger intragroup variation. Subtle time effects in the recovery process were displayed along the third component, even though these coordinates were heavily overlapped. However, there was less overlap in recovery time points of the 48 h transport group as compared to the 12 h transport group. The recovery samples of the sheep transported for 48 h exhibited higher levels of the branched-chain amino acids (BCAA), valine, leucine and isoleucine.

A PLS-DA model of pretransport and arrival serum samples was computed (Table 1, M6) to scrutinize the perturbations induced by the transport event. Pretransport and arrival samples

**Table 2.** VIP (Variable Importance in the Projection) Values of Key Metabolites As Derived from PLS-DA Analysis<sup>a</sup>

	VIP		
	48 h	12 h	Pre+Arr
urinary metabolites			
4-cresol sulfate	3.21	3.78	4.23
Acetoacetate	0.78	1.74	1.60
Azelate	1.48	1.48	0.81
Betaine	5.08	2.95	1.46
Crotonyl glycine	1.28	0.90	1.47
CG+TG	1.69	1.47	1.64
Citrate	0.93	1.03	0.70
Creatine	3.95	3.29	4.18
Creatinine	3.12	2.49	3.69
Free fatty acids	1.13	1.08	1.03
Hippurate	3.78	3.78	3.84
N-isovalerylglycine	1.60	1.61	1.12
Lactate	1.33	2.51	1.10
O-acetyl carnitine	1.04	1.21	0.75
O-phosphocholine	0.97	2.19	1.38
Phenylacetyl glycine	2.83	3.01	3.21
Propane 1,2-diol	1.84	0.71	0.56
UmA	2.83	3.45	2.15
UmB	1.90	1.65	0.83
UmC	0.96	0.67	1.14
serum metabolites			
3-hydroxybutyrate	2.61	1.04	2.69
Acetate	4.08	4.33	4.78
Acetone	1.07	0.62	1.89
BCAA	4.18	6.12	2.24
Betaine	7.36	5.33	7.93
Citrate	1.05	1.28	0.91
Creatine	2.02	0.96	1.34
Glucose	1.29	1.36	1.66
LDL/VLDLs	4.15	3.68	4.08
N-acetyl glycoproteins	3.23	2.63	3.49
Phosphatidylcholine	4.11	3.97	3.85

<sup>a</sup> VIP values of the PLS-DA of urines and sera of all the time points of the 48 h transport group, of the 12 h transport group and those derived from the PLS-DA models of pre-transport and arrival (Pre+Arr) samples only are presented. Variables with VIP > 1 are of significance. See Figure 2 legend for metabolite abbreviations.

are clearly separated along the first component ( $t_1$ ) in the scores plot (Figure 4C). Similar to the urinary profiles, the metabolic profiles of the arrival serum samples after 48 h transport are distinct along the second component ( $t_2$ ) from the corresponding arrival samples from the group transported for 12 h. The loadings plot (Figure 4D) and the changes of relative concentrations (Table 3) indicated that the levels of LDL/VLDLs, phosphatidylcholine, acetate and citrate declined and the levels of glucose, and N-acetyl glycoproteins increased after transport in both treatments. The 48 h transport treatment induced further changes to the serum metabolic profiles compared to 12 h transport. In addition, levels of betaine, creatine, acetone, and 3-hydroxybutyrate also significantly increased after 48 h transport. Collectively, these data demonstrated that the

longer duration transport caused different perturbations to the animals' metabolism compared to the 12 h transport event.

The metabolic trajectories as captured by the five time points (Table 1, M8) exhibited time effects with the longer transport treatment establishing an extended trajectory (Figure 5B), similar to the pattern in urine (Figure 5A). As with the trajectories developed for the urine samples, the greatest changes were observed between the first 3 time points, with convergence to a new state through recovery.

### O2PLS Analysis of Urine and Serum Samples

O2PLS analyses were performed on bucketed urine and serum spectra to investigate correlations between both data sets, and results are displayed in Figure 6. In both transport cohorts, urinary hippurate, phenylacetyl glycine, betaine, creatine, creatinine, and 4-cresol sulfate were highly correlated with acetate, creatine, betaine and citrate in serum (Figure 6A and B). After 48 h transport, the correlation coefficients of urinary crotonyl glycine, tiglylglycine, UmC, and propane 1,2-diol with serum creatine, acetone, and acetate were increased when compared with the 12 h transported (Figure 6A and B). This demonstrates that the 48 and 12 h transports had different effects on the perturbation of metabolic profiles.

## DISCUSSION

Road transport of livestock raises welfare and productivity concerns for animal production industries and presents metabolic challenges to the animals through feed and water deprivation, muscle fatigue and stress hormone responses to changed social and physical environments. Previous studies of road transport report weight loss as the major impact of most transport events, and indeed in this experiment, the sheep transported for 12 h lost an average of approximately 5% bodyweight, while the group transported for 48 h lost an average of 12% bodyweight.<sup>22</sup> Much of this loss is due to ruminal and intestinal emptying since daily feed intake contributes to about 4% of bodyweight.<sup>21,34</sup> Increased serum free fatty acids (FFA) and 3-hydroxybutyrate are consistently reported,<sup>21,35</sup> while both increases and decreases of serum glucose have been observed in different transport experiments.<sup>19</sup> Studies of sheep fasted for 2–3 days found increased serum FFA and 3-hydroxybutyrate and decreased serum glucose.<sup>19,20,36</sup>

While clinical biochemistry indicators detect gross metabolic changes, these assays are not sensitive to the more subtle metabolic adaptations or variations in transport treatments. Indeed, Fisher et al.<sup>22</sup> found no statistical differences between the metabolic responses induced by 12, 30, and 48 h of continuous road transport of sheep. We conducted this metabonomics study on both the urine and serum samples on the two cohorts of sheep ( $n = 40$ ) transported for 12 and 48 h to determine if NMR-based metabonomics could discriminate between the metabolic responses induced by the different transport durations, and describe in detail the recovery trajectories in each case. Significant metabolites are discussed below according their occurrence in major metabolic pathways as annotated by the Kyoto Encyclopedia of Genes and Genomes.<sup>37</sup>

### Changes in Carbohydrate Metabolism after Road Transport

The increased levels of serum glucose of the animals transported for 12 h was indicative of glycolysis through the mobilization of liver glycogen stores. Conversion of glucose to pyruvate supplied immediate energy through the Krebs cycle, with excess pyruvate converted to lactate for gluconeogenesis or excreted via

Table 3. Changes in Key Metabolites over Time Analyzed by Linear Mixed Effect Models<sup>a</sup>

metabolite	transport duration	recovery						increment		recovery	
		pretransport	arrival	24 h	48 h	72 h	$(\mu_{12\text{ h}} - 0)$	$(\mu_{48\text{ h}} - \mu_{12\text{ h}})$	trend <sub>12 h</sub>	trend <sub>48 h</sub>	
Carbohydrate metabolism											
Acetate	12 h*	0.88 ± 0.19	0.63 ± 0.09	0.77 ± 0.16	0.79 ± 0.15	0.72 ± 0.13	---	0/0	+	++	
	48 h*	0.71 ± 0.18	0.45 ± 0.06	0.70 ± 0.15	0.83 ± 0.20	0.72 ± 0.15	---	---			
Citrate	12 h	0.17 ± 0.05	0.21 ± 0.07	0.25 ± 0.07	0.20 ± 0.03	0.19 ± 0.02	+++/+++	0/--	0/--	0/0	
	48 h	0.14 ± 0.01	0.17 ± 0.02	0.32 ± 0.28	0.28 ± 0.15	0.23 ± 0.13					
	12 h*	0.24 ± 0.03	0.20 ± 0.03	0.17 ± 0.02	0.18 ± 0.03	0.19 ± 0.03	---	---	0	++	
	48 h*	0.22 ± 0.02	0.16 ± 0.02	0.18 ± 0.03	0.18 ± 0.03	0.20 ± 0.03					
Glucose	12 h*	0.74 ± 0.05	0.89 ± 0.07	0.85 ± 0.06	0.83 ± 0.05	0.82 ± 0.05	+++	-	-	-	
	48 h*	0.80 ± 0.07	0.90 ± 0.08	0.84 ± 0.05	0.83 ± 0.06	0.86 ± 0.07					
Lactate	12 h	0.28 ± 0.18	0.61 ± 1.18	0.67 ± 0.51	0.41 ± 0.20	0.40 ± 0.11	+	0	0/0	0/0	
	48 h	0.27 ± 0.14	0.40 ± 0.38	0.38 ± 0.20	0.45 ± 0.25	0.48 ± 0.42					
Propane 1,2-diol	12 h	0.36 ± 0.18	0.39 ± 0.26	0.46 ± 0.22	0.45 ± 0.31	0.42 ± 0.32	0	0	0	0	
	48 h	0.25 ± 0.10	0.32 ± 0.21	0.45 ± 0.29	0.59 ± 0.42	0.37 ± 0.16					
Lipid metabolism											
3-hydroxybutyrate	12 h*	1.14 ± 0.07	1.11 ± 0.09	1.13 ± 0.08	1.14 ± 0.11	1.14 ± 0.11	0/0	0/+++	0	++	
	48 h*	1.10 ± 0.09	1.18 ± 0.17	1.20 ± 0.15	1.07 ± 0.11	1.12 ± 0.11					
Acetoacetate	12 h	0.35 ± 0.06	0.67 ± 0.11	0.44 ± 0.06	0.47 ± 0.08	0.53 ± 0.09	+++/+++	-/-	-	--	
	48 h	0.34 ± 0.06	0.57 ± 0.09	0.37 ± 0.08	0.40 ± 0.06	0.43 ± 0.07					
Acetone	12 h*	0.29 ± 0.04	0.30 ± 0.04	0.27 ± 0.02	0.29 ± 0.02	0.30 ± 0.03	+	+++	-	0	
	48 h*	0.24 ± 0.02	0.28 ± 0.04	0.31 ± 0.05	0.29 ± 0.02	0.30 ± 0.02					
Azelate	12 h	0.28 ± 0.07	0.29 ± 0.07	0.43 ± 0.05	0.46 ± 0.07	0.46 ± 0.08	+/0	0/0	+	++	
	48 h	0.23 ± 0.03	0.26 ± 0.04	0.37 ± 0.05	0.44 ± 0.05	0.43 ± 0.07					
CG+TG	12 h	0.36 ± 0.06	0.54 ± 0.16	0.43 ± 0.09	0.42 ± 0.07	0.45 ± 0.09	+++	+++	0	--	
	48 h	0.38 ± 0.06	1.06 ± 0.24	0.53 ± 0.20	0.42 ± 0.14	0.45 ± 0.15					
Free fatty acids	12 h	0.14 ± 0.04	0.09 ± 0.02	0.16 ± 0.02	0.18 ± 0.03	0.17 ± 0.02	---	0/+++	+	++	
	48 h	0.10 ± 0.01	0.07 ± 0.01	0.16 ± 0.03	0.20 ± 0.03	0.19 ± 0.03					
LDL/VLDLs	12 h*	1.91 ± 0.20	1.58 ± 0.21	1.71 ± 0.19	1.70 ± 0.19	1.65 ± 0.20	---	-/0	+	++	
	48 h*	1.81 ± 0.25	1.42 ± 0.20	1.59 ± 0.21	1.54 ± 0.19	1.56 ± 0.22					
O-acetyl carnitine	12 h	0.17 ± 0.03	0.30 ± 0.27	0.26 ± 0.08	0.21 ± 0.04	0.22 ± 0.06	0/+++	++/0	0/-	--/	
	48 h	0.16 ± 0.03	0.34 ± 0.17	0.37 ± 0.19	0.26 ± 0.08	0.21 ± 0.07					
Glycerolipid and glycerophospholipid metabolism											
Betaine	12 h	0.87 ± 0.68	1.03 ± 0.86	1.40 ± 0.50	1.19 ± 0.49	0.96 ± 0.56	0/0	+++/0	0/0	--/0	
	48 h	0.66 ± 0.47	2.06 ± 1.71	4.09 ± 2.22	1.94 ± 1.06	1.14 ± 0.64					
O-phosphocholine	12 h*	1.59 ± 0.20	1.60 ± 0.19	1.72 ± 0.27	1.72 ± 0.29	1.71 ± 0.32	0/0	+++/+++	0/+	--/-	
	48 h*	1.68 ± 0.23	2.18 ± 0.37	2.13 ± 0.33	1.73 ± 0.35	1.61 ± 0.30					
Phosphatidylcholine	12 h	0.13 ± 0.03	0.47 ± 0.87	0.25 ± 0.31	0.19 ± 0.05	0.20 ± 0.06	++	0	0/0	0/0	
	48 h	0.13 ± 0.07	0.22 ± 0.10	0.31 ± 0.19	0.27 ± 0.12	0.19 ± 0.06					
4-cresol sulfate	12 h*	2.10 ± 0.19	1.90 ± 0.19	2.10 ± 0.18	2.04 ± 0.18	1.97 ± 0.17	---	---/0	0	++	
	48 h*	1.98 ± 0.21	1.67 ± 0.20	1.94 ± 0.20	1.89 ± 0.14	1.82 ± 0.15					
Gut microbiome cometabolites											
Hippurate	12 h	4.46 ± 0.66	1.86 ± 0.51	2.10 ± 0.48	2.30 ± 0.68	1.57 ± 0.58	---	---/---	+	+	
	48 h	5.22 ± 1.15	0.50 ± 0.20	2.14 ± 0.68	2.67 ± 0.93	2.26 ± 0.79					

Table 3. Continued

metabolite	transport duration	recovery						increment		recovery	
		pretransport	arrival	24 h	48 h	72 h	$(\mu_{12 \text{ h}} - 0)$	$(\mu_{48 \text{ h}} - \mu_{12 \text{ h}})$	trend <sub>12 h</sub>	trend <sub>48 h</sub>	
Phenylacetylglycine	12 h	3.00 ± 0.39	4.20 ± 0.34	3.18 ± 0.43	3.30 ± 0.49	3.73 ± 0.52	+++/+++	0/0	--	0	
	48 h	2.39 ± 0.53	3.70 ± 0.43	2.19 ± 0.65	2.57 ± 0.73	3.32 ± 0.77					
Creatine metabolism											
Creatine	12 h	1.48 ± 0.53	2.82 ± 0.83	3.19 ± 0.77	2.93 ± 0.89	2.90 ± 0.77	+++/+++	+++/+++	0	-	
	48 h	1.80 ± 0.63	6.23 ± 1.66	2.70 ± 0.73	2.60 ± 0.59	3.22 ± 0.85					
	12 h*	0.80 ± 0.05	0.79 ± 0.06	0.80 ± 0.05	0.80 ± 0.05	0.79 ± 0.05	0/0	+++/+++	0/0	--/0	
	48 h*	0.78 ± 0.06	0.87 ± 0.06	0.80 ± 0.05	0.78 ± 0.06	0.80 ± 0.07					
Creatinine	12 h	2.61 ± 0.55	3.43 ± 0.51	3.40 ± 0.50	3.17 ± 0.59	3.36 ± 0.61	+++/+++	+++/+++	0	--	
	48 h	2.97 ± 0.78	5.81 ± 0.59	3.52 ± 0.99	3.22 ± 0.86	3.44 ± 0.81					
Branched chain amino acid metabolism											
BCAA	12 h*	1.11 ± 0.06	1.10 ± 0.06	1.30 ± 0.11	1.39 ± 0.15	1.40 ± 0.15	0/0	0/-/-	+	+	
N-isovalerylglycine	48 h*	1.17 ± 0.11	1.14 ± 0.07	1.29 ± 0.08	1.44 ± 0.14	1.38 ± 0.13					
	12 h	0.43 ± 0.08	0.43 ± 0.07	0.61 ± 0.08	0.64 ± 0.10	0.66 ± 0.15	++±--	+++/+++	+	++	
	48 h	0.37 ± 0.05	0.57 ± 0.10	0.56 ± 0.07	0.67 ± 0.08	0.63 ± 0.09					
Other metabolites											
N-acetyl glycoproteins	12 h*	1.51 ± 0.12	1.56 ± 0.11	1.52 ± 0.10	1.55 ± 0.11	1.56 ± 0.12	++/++	++/++	0	0	
	48 h*	1.45 ± 0.09	1.62 ± 0.11	1.59 ± 0.09	1.58 ± 0.09	1.60 ± 0.10					
UmA	12 h	0.36 ± 0.36	0.60 ± 0.60	0.60 ± 0.41	0.23 ± 0.12	0.16 ± 0.03	0/+++	0/-/-	0/-/-	0/0	
	48 h	0.11 ± 0.02	0.09 ± 0.01	0.92 ± 0.48	0.70 ± 0.56	0.26 ± 0.14					
UmB	12 h	0.12 ± 0.03	0.17 ± 0.07	0.29 ± 0.08	0.25 ± 0.07	0.22 ± 0.07	++/++	---/---	+	++	
	48 h	0.11 ± 0.01	0.08 ± 0.01	0.25 ± 0.09	0.38 ± 0.13	0.41 ± 0.15					
UmC	12 h	0.20 ± 0.03	0.22 ± 0.05	0.24 ± 0.03	0.24 ± 0.03	0.25 ± 0.03	+/0	++/++	0	--	
	48 h	0.19 ± 0.03	0.46 ± 0.12	0.29 ± 0.10	0.26 ± 0.05	0.26 ± 0.06					

<sup>a</sup>Data were obtained by using relative intensity of variables (scaled by total sum intensity (minus exclusion zones) of spectra) at the time points of pretransport, arrival, and 24 h, 48 h, and 72 h recovery. Univariate analysis via linear mixed effect models was performed for each of the metabolites identified in the multivariate analysis as significant. The increment in metabolite concentration for a 12 h transport as well as any additional increment for a 48 h transport was tested for significance. The direction of the increment is indicated by (-,+) and the level of significance by the number of symbols, e.g., +: 0.05, ++: 0.01, +++: 0.001. Where a significant block and/or interaction effect was observed, the values are reported separately for the first and second block, e.g., 0/++, showing no significant effect in first replicate and a significant effect in the second replicate. For the recovery trend, the direction of any significant trend is indicated by (-,+). A trend is deemed significant if the corresponding approximate t test value is greater than 2. If the block effect could not be ignored separate values are reported for each block. If no block effect was observed, “++” or “--” is used to indicate if one treatment has a significant larger slope. Serum metabolites are indicated by asterisks (\*).

urine. Urinary lactate was markedly increased although levels of excretion were highly variable across the arrival samples of this group. In contrast, after 48 h transport, the sheep were less dependent on glycolysis; while serum glucose and urinary lactate were increased, their levels were lower than the corresponding 12 h arrival samples. The decreased serum acetate on arrival in both groups implied limited conversion of acetyl-CoA to acetate.

Recovery commenced once animals were off-loaded from the transport vehicles and allowed *ad libitum* food and water. The animals transported for 12 h responded rapidly to cessation of transport. By 24 h post-transport, the liver had returned to reliance on the TCA cycle, and the animals remained glycolytic and gluconeogenic (apparent from the persistence of high levels serum glucose and urine lactate). The concentrations of serum glucose of the animals transported for 48 h also returned to pretransport values at 24 h recovery, but high urinary lactate levels persisted suggesting that gluconeogenesis (via lactate) was reduced as the intake of food provided propionate as an energy source. A “recovery specific” metabolite, propane 1,2-diol, achieved maximum excretion at 48 h recovery in the urine of the animals transported for 48 h. Although, it is not significant in the univariate

analysis (Table 3), its presence may still potentially indicate spillover of excess lactate via its conversion to lactaldehyde.

### Changes in Lipid Metabolism after Road Transport

After 12 h transport, there was increased levels of urinary acetoacetate and *O*-acetyl carnitine, both indicative of some utility of circulating lipids; however, the markers of ketosis, serum 3-hydroxybutyrate and acetone were not changed. In contrast, after 48 h transport, the animals were clearly mobilizing and utilizing adipose stores. Urine acetoacetate, and the serum ketotic indicators, 3-hydroxybutyrate and acetone were increased on arrival; however, these animals were not clinically ketotic.<sup>22</sup> Urinary *O*-acetyl carnitine concentrations were also markedly increased in the 48 h transport group; consistent with studies of fasting human subjects where *O*-acetyl carnitine was excreted in the ketotic phase.<sup>17,38</sup> By 24 h post-transport, decisive falls to near pretransport levels were observed for all urinary indicators of fatty acid metabolism. However, fatty acid mobilization and ketogenesis were still operative in the group transported for 48 h (i.e., serum acetone and urine *O*-acetyl carnitine remained at increased levels).

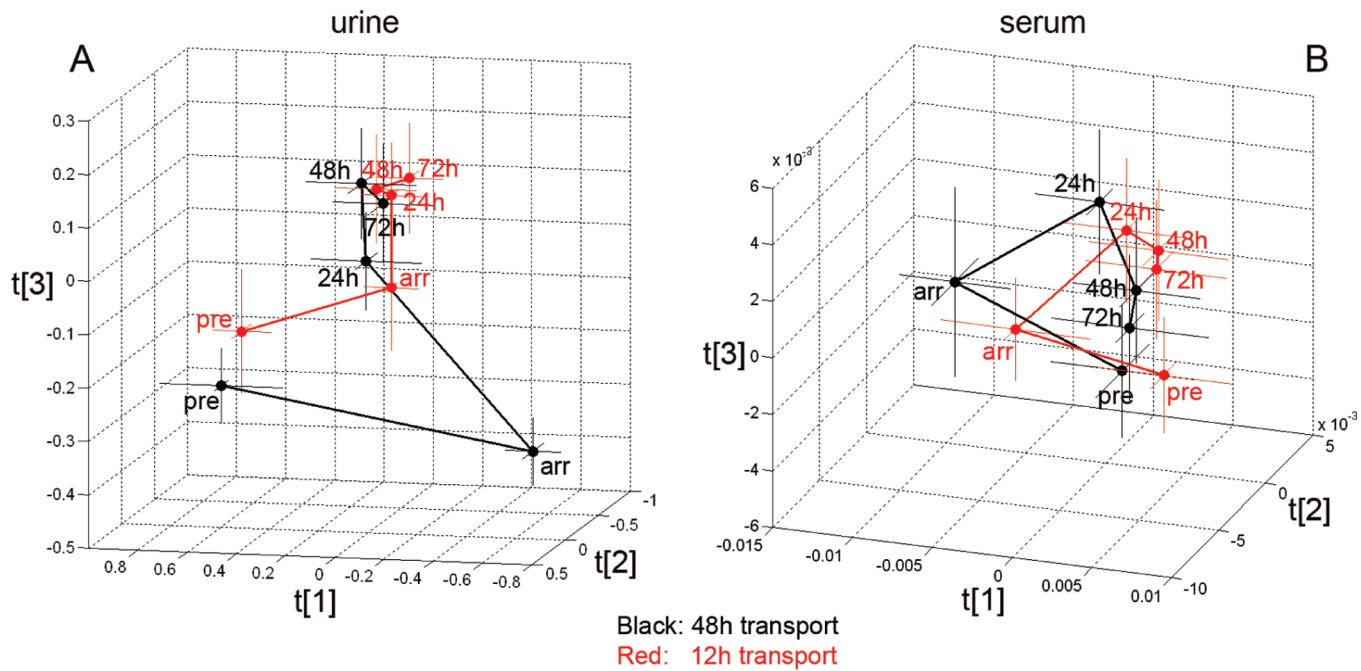


**Figure 5.** Metabolic trajectories through the transport treatment and recovery period. Panel A: the trajectories of urine metabolic profiles of the 12 and 48 h transported groups ( $R^2X[1] = 0.366$ ,  $R^2X[2] = 0.154$ ,  $R^2X[3] = 0.121$ ,  $R^2Y = 0.405$ ,  $Q^2 = 0.399$ ); and Panel B: the trajectories of serum metabolic profiles of the 12 and 48 h transported groups ( $R^2X[1] = 0.364$ ,  $R^2X[2] = 0.116$ ,  $R^2X[3] = 0.105$ ,  $R^2Y = 0.313$ ,  $Q^2 = 0.299$ ). Mean values and standard deviations of each group are shown. Data were obtained from PLS-DA analysis of urine and serum spectra. Abbreviations: pre, pretransport; arr, arrival; 24 h, 24 h post-transport; 48 h, 48 h post-transport; 72 h, 72 h post-transport.

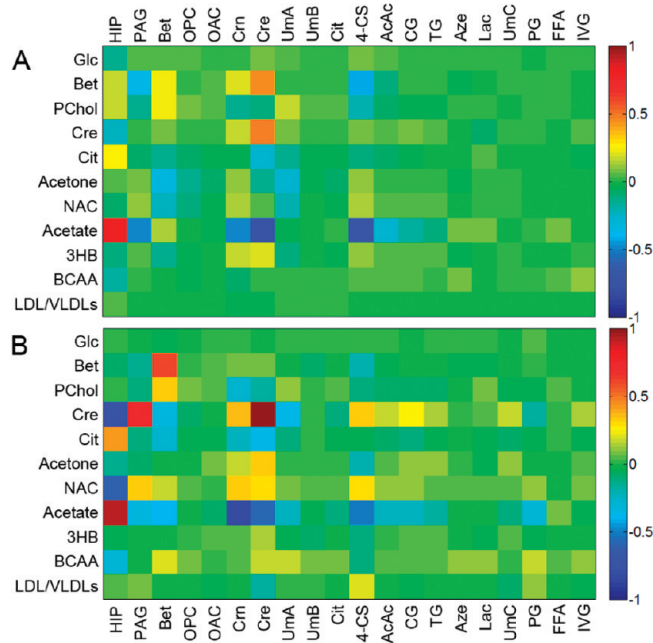


**Figure 6.** Coefficients of O<sub>2</sub>PLS analysis of urinary and serum key metabolites. Panels A and B: Correlations between urinary and serum metabolites from sheep transported for 12 and 48 h, respectively. Horizontal axis, urinary metabolites; Vertical axis, serum metabolites. See Figure 2 legend for metabolite abbreviations.

Two short chained acyl glycine conjugates, crotonyl glycine and tiglylglycine, were increased in urine of the arrival samples of both groups, with the 48 h transport group exhibiting markedly increased excretion of these two metabolites. These acyl glycine

conjugates and O-acetylcarnitine are byproducts of incomplete  $\beta$ -oxidation of fatty acids. The  $\beta$ -oxidation fatty acid oxidation pathway functions in both the mitochondria and peroxisomes, with the minor  $\omega$ -oxidation pathway also functioning within peroxisomes and microsomes.<sup>39,40</sup> Acyl glycines are commonly detected in humans with deficiencies or defects of peroxisomal and/or mitochondrial enzymes.<sup>41,42</sup> The excretory profile of UmC paralleled that of crotonyl glycine and tiglylglycine, suggesting that it may arise from the same pathways as the acyl glycine conjugates.

Curiously, increasing excretion of azelate, a medium chain (C9) dicarboxylic acid, was detected for both groups of animals throughout the recovery period, despite the excretion of acyl glycines, tiglylglycine and crotonyl glycine, returning to near normal levels. Dicarboxylic aciduria is associated with altered fatty acid metabolism due to glycogen storage diseases, ketosis, and drug induced mitochondrial damage.<sup>43–45</sup>

#### Changes in Glycerolipid and Glycerophospholipid Metabolism after Road Transport

In the group transported for 12 h, levels of serum betaine and urine O-phosphocholine were increased, while both urine and serum betaine are markedly increased after 48 h transport. Urine betaine achieved maximum excretion at 24 h post-transport and then rapidly recovered. Betaine is the product of oxidation of choline in the liver and kidney. In the liver, it can act as a cytoplasmic methyl donor. Additionally, kidney mitochondria very efficiently import choline for conversion to betaine<sup>46</sup> where it functions, along with glycerophosphocholine, as a compensatory osmolyte in the renal medulla experiencing high urea or salt.<sup>47</sup> The contribution of each organ to the production of betaine in fasting ruminants is not known, especially taking into account that in sheep, muscle and brain are also sources of choline.<sup>48</sup>

As previous mentioned, propane 1,2-diol, achieved maximum excretion at 48 h recovery in the urine of the animals transported for 48 h. This metabolite may also be a byproduct of excess glycerol as a consequence of the release of fatty acid moieties and glycerol from triacylglycerols transported to and processed in the liver. However, there maybe a renal contribution, since glycerol is a by-product of choline and alpha-glycerophosphate degradation, which are in turn, degradation products of glycerophosphocholine

### Changes in Gut Microbiome Cometabolites after Road Transport

Urinary hippurate was depressed on arrival in both groups and markedly decreased (by 90%) in urine of the 48 h group, and levels of phenylacetylglycine and 4-cresol sulfate were significantly increased. Hippurate, phenylacetylglycine and 4-cresol sulfate are mammalian-gut microbiome cometabolites and can act as urinary indicators of gut metabolism. Hippurate and phenylacetylglycine are the glycine conjugates of benzoic acid and phenylacetic acid respectively. 4-Cresol sulfate is the sulphated conjugate of 4-cresol. Benzoic acid is derived from rumen catabolism of dietary phenolics,<sup>49–51</sup> while phenylacetic acid and 4-cresol are products of microbial processing of dietary and endogenously derived phenylalanine and tyrosine respectively, which are released by gut proteolytic processes.<sup>52,53</sup>

Rumen function is known to virtually cease with 24 h feed and water deprivation.<sup>21</sup> The excretion of the cometabolites reflected the reduced dietary substrate in the rumen and intestine, and the altered microbial populations due to fasting and increased relative protein content from normal and possibly increased gut epithelial turnover. 4-Cresol levels are known to increase in the gut with fasting<sup>54</sup> and increased urinary excretion of phenylacetylglycine and/or 4-cresol sulfate are associated with a numerous conditions with altered gut metabolism and microbiota.

At 24 h recovery and after food intake, urinary hippurate returned to approximately half pretransport output and phenylacetylglycine and 4-cresol sulfate returned to pretransport levels in both groups of animals. However, the excretion of phenylacetylglycine and 4-cresol sulfate proceeded to increase over the next 48 h indicating that gut metabolism had not stabilized at this time. Fasted sheep eat to satiety on first intake, rehydrate and then consume little food for next 2 days.<sup>19</sup> Moreover, after 48–96 h fast, normal rumen function requires 6–12 days to fully re-establish.<sup>21,60</sup>

### Changes in Creatine Metabolism after Road Transport

After 12 h transport, levels of urinary creatine and creatinine were increased, but serum creatine was unchanged indicating that no excessive muscle catabolism had occurred. In contrast, 48 h transport caused increased serum creatine levels and induced marked increases in concentrations of urinary creatinine and creatine. Increased urinary levels of creatine and creatinine imply some physical exertion and/or leakage from muscle. Serum creatine increases in fasting due to decreased uptake of creatine by skeletal muscle and increased mobilization of creatine to the kidney.<sup>61</sup> Muscle catabolism was still active in both transport groups during recovery. Both urinary creatine and creatine remained at a plateau (above pretransport levels).

### Changes in Branched Chain Amino Acid Metabolism after Road Transport

Along with increasing serum BCAA levels over the recovery period, there is a concomitant rise in urine *N*-isovalerylglycine which probably reflected increased hepatic oxidation of leucine.<sup>62</sup>

Serum BCAA levels increase with starvation, nutritional and diabetic perturbations of metabolism.<sup>62–64</sup> In fasting animals, increased serum BCAA levels are attributed to decreased hepatic uptake and oxidation of the BCAA on their release from protein by muscle catabolism.<sup>62,64,65</sup> High serum ketone bodies also acts on skeletal muscle to decrease oxidation of BCAA.<sup>66</sup>

### UmA

Unknown urine metabolite, UmA, achieved high levels at 24 h recovery, and along with urine betaine, is one of the most sensitive metabolites to recovery and food intake. Identification of UmA should reveal which metabolic pathway, organelle(s) and organ is responding to the stressors of transport.

### Functional Assessment of the Metabolic Perturbations

The models developed from the NMR-based metabonomics analyses of both serum and urinary metabolic profiles have demonstrated a clear difference between the two transport durations and the recovery from the metabolic perturbation induced by the treatments. The metabolic perturbation experienced by the sheep transported for 12 h was less intense or extensive than that experienced by the animals transported for 48 h. However, the metabolic perturbation of the animals during the 48 h transport is not merely an extension of the response over 12 h transport, as evidenced by the average metabolic trajectories depicted in Figure 5: The 48 h transport group exhibited a very different and more complex metabolic trajectory. The animals on arrival after 48 h transport are located in a section of metabolic space that is not just different from the 12 h animals but also in a different direction from the starting point. This means that the metabolic response of the animals during the transport is biphasic and that the metabolic events between 12 and 48 h are different than during the first 12 h of transport. This behavior is also underlined by the results from the univariate linear modeling, as presented in Table 3. Several metabolites, mostly connected to lipid metabolism, exhibit a biphasic behavior of either increasing during 12 h of transport but then decreasing between 12 and 48 h or vice versa. The later time points indicated convergence of both transport groups to a new and similar metabolic state, indicating that the metabolic disturbance during both transport durations is “mild” enough to allow recovery over 72 h, and reflecting the fact that the animals are under identical conditions during recovery. The study also highlighted the role of urine as a repository of “excess” metabolites and thus the value of urine collection for metabonomic studies.

As highlighted above, the strongest difference between the responses to transport was apparent in the metabolic states on arrival. The animals transported for 48 h were clearly ketogenic, and other hepatic responses were indicated by distinctively high signals from crotonyl glycine/tiglylglycine and possibly UmA. A twelve hour fast by ruminants is not metabolically onerous; however a 12 h deprivation of food and water under road transport conditions may be approaching the limits of the primary adaptive responses of glycolysis of glycogen stores, gluconeogenesis and consumption of circulating lipid. Furthermore, the metabolic profiles of the 48 h transport group on arrival and through recovery were characterized by markedly increased urinary excretion of creatine, creatinine, betaine, citrate and O-phosphocholine. This urinary profile is similar to that obtained from patients suffering polymyositis, a condition of chronic inflammation of skeletal muscle.<sup>67</sup> Impacts on meat quality with this level of muscle inflammation must be anticipated. The rapid return to near normal excretion of creatinine, creatine and crotonyl glycine/tiglylglycine on

cessation of transport demonstrated the resilience of both skeletal muscle and hepatic compartments in these ruminants; however, it does not provide insight as to the resilience required of long duration transport animals arriving into totally new environments such as feedlots and saleyards where change of diet, handling and increased exposure to infectious disease are experienced.

NMR-based metabolomics studies of fasting experiments and various stress models in humans and rodents have reported degrees of changes in many of the serum and urine metabolites that we have observed.<sup>6,14,18,68</sup> Our analyses points to the complexities of energy metabolism both during the transport event where the animals will have developed some level of adaptation, and during the subsequent recovery phase. Sustained urinary excretion of significantly elevated levels of intermediate and end point products from peroxisomal and microsomal fatty acid oxidation was unexpected, and indicates an altered relationship between these organelles and the mitochondria in the processing of fatty acids mobilized from adipose stores into the liver. There are two peroxisomal fatty acid oxidation systems that augment cellular ability to process a wide range of substrates including very long chain fatty acids, long chain dicarboxylic acid, hydroxyl fatty acids and branched chain fatty acids.<sup>40,69,70</sup> Excretion of short and medium chain dicarboxylic acids (such as azelic acid) is likely due to the incomplete  $\beta$ -oxidation in the peroxisome of long chain dicarboxylic acyl fatty acids derived from microsomal  $\omega$ -oxidation.<sup>40,70</sup> In addition, the acyl glycines, crotonyl glycine and tiglylglycine, whose elevated excretion was a major differentiator between the two transport groups, are also the end-products of the incomplete  $\beta$ -oxidation in the peroxisome followed by peroxisomal acyl-CoA thioesterase (ACOT) processing of crotonic acid and tiglic acid. Both are small unsaturated monocarboxylic acids; tiglic acid is also methyl branched. A portion of small to medium dicarboxylic acids is also destined to be glycine conjugated in the peroxisome prior to excretion.<sup>70</sup>

The peroxisome would appear to be a significant site for the metabolic expression of adaptation to stress and subsequent recovery, and the ruminant peroxisome may have evolved a different "job sharing" relationship with the mitochondria compared to that described for rodents.<sup>71</sup> Indeed, differences in peroxisomal  $\beta$  fatty acid oxidization is observed between species, with larger mammals (humans and cattle) possessing higher peroxisomal fatty acid oxidative activity in skeletal muscle than rats.<sup>72,73</sup> More insights into this question can be derived from analyses of the recently assembled cattle and sheep genome sequences. A preliminary analysis of bovine type I ACOT genes revealed a cluster of six genes. Unlike the orthologous genes in the mouse and human, all six of the putative bovine ACOTs are tagged for import into peroxisomes (unpublished data). In contrast, the human and mouse counterparts are targeted specifically to either the microsomes, mitochondria or peroxisomes.<sup>70</sup>

NMR-based metabolomics at its current stage of development can give indications of system-wide metabolic perturbations, thus directing enquiry to organs and organelles active in stress response. With deeper analysis of both the biology at this level and use of sensitive and targeted technologies, such as mass spectrometry based metabolomics, we can hope to identify very sensitive and true indicators of stress response and recovery, as predictive tools of health and well being.

## ■ ASSOCIATED CONTENT

### Supporting Information

Supplementary tables and figures. This material is available free of charge via the Internet at <http://pubs.acs.org>.

## ■ AUTHOR INFORMATION

### Corresponding Author

\*Tel: +61 (0)7 3214 2510. Fax: +61 (0)7 3214 2900. E-mail: Gene.Wijffels@csiro.au.

### Present Addresses

<sup>†</sup>Faculty of Veterinary Science, The University of Melbourne, Corner Park Drive and Flemington Road, Parkville, Vic 3052, Australia.

## ■ ACKNOWLEDGMENT

We are very grateful to Drs Alan Bell, Dean Revell, Ross Tellam and Nick Hudson for useful discussions on ruminant metabolism and critique. NMR spectra were measured in the NMR facility of the Institute for Molecular Bioscience at the University of Queensland. J.L. was a recipient of a Ph.D. student scholarship from the Chinese Scholarship Council.

## ■ ABBREVIATIONS

1/2/3D, 1/2/3-dimensional; 3HB, 3-hydroxybutyrate; AcAc, acetacetate; Ala, alanine; Aze, azelate; BCAA, branched-chain amino acids; Bet, betaine; Cit, citrate; Cre, creatine; Crn, creatinine; CG, crotonyl glycine; DCA, dicarboxylic acid; DQF-COSY, double-quantum filtered correlation spectroscopy; DMA, dimethylamine; DFTMP, 1,1-difluoro-1-trimethylsilyl methyl phosphanic acid; DSS, 2,2-dimethyl-2-sila-3,3,4,4,S,S-hexadeuteropentane-5-sulfonic acid; Glc, glucose; HIP, hippurate; HMBC, heteronuclear multiple bond correlation; HSQC, heteronuclear single quantum coherence; IVG, N-isovalerylglycine; Lac, lactate; LDL/VLDLs, low/very low density lipoproteins; MVSA, multivariate statistical analysis; NAC, N-acetyl glycoproteins; OAC, O-acetyl carnitine; OPC, O-phosphocholine; PAG, phenylacetylglycine; PCA, principle components analysis; PChol, phosphatidylcholine; PG, propane 1,2-diol; PLS-DA, partial least-squares-discriminant analysis; TG, tiglylglycine; TMAO, trimethylamine N-oxide; TOCSY, total correlation spectroscopy; TPPI, time-proportional phase incrementation; UmA/B/C, unidentified metabolite A/B/C; UV, univariance

## ■ REFERENCES

- (1) Nicholson, J. K.; Lindon, J. C.; Holmes, E. 'Metabonomics': understanding the metabolic responses of living systems to pathophysiological stimuli via multivariate statistical analysis of biological NMR spectroscopic data. *Xenobiotica* **1999**, *29* (11), 1181–1189.
- (2) Salek, R. M.; Xia, J.; Innes, A.; Sweatman, B. C.; Adalbert, R.; Randle, S.; McGowan, E.; Emson, P. C.; Griffin, J. L. A metabolomic study of the CRND8 transgenic mouse model of Alzheimer's disease. *Neurochem. Int.* **2010**, *56* (8), 937–947.
- (3) Sun, J.; Schnackenberg, L. K.; Holland, R. D.; Schmitt, T. C.; Cantor, G. H.; Dragan, Y. R.; Beger, R. D. Metabonomics evaluation of urine from rats given acute and chronic doses of acetaminophen using NMR and UPLC/MS. *J. Chromatogr., B: Anal. Technol. Biomed. Life Sci.* **2008**, *871* (2), 328–340.
- (4) Bertram, H. C.; Kristensen, N. B.; Vestergaard, M.; Jensen, S. K.; Sehested, J.; Nielsen, N. C.; Malmendal, A. Metabolic characterization of

- rumen epithelial tissue from dairy calves fed different starter diets using  $^1\text{H}$  NMR spectroscopy. *Livest. Sci.* **2009**, *120* (1–2), 127–134.
- (5) Yan, B.; A, J. Y.; Wang, G. J.; Lu, H. L.; Huang, X. P.; Liu, Y.; Zha, W. B.; Hao, H. P.; Zhang, Y.; Liu, L. S.; Gu, S. H.; Huang, Q.; Zheng, Y. T.; Sun, J. G. Metabolomic investigation into variation of endogenous metabolites in professional athletes subject to strength-endurance training. *J. Appl. Physiol.* **2009**, *106* (2), 531–538.
- (6) Teague, C. R.; Dhabhar, F. S.; Barton, R. H.; Beckwith-Hall, B.; Powell, J.; Cobain, M.; Singer, B.; McEwen, B. S.; Lindon, J. C.; Nicholson, J. K.; Holmes, E. Metabonomic studies on the physiological effects of acute and chronic psychological stress in Sprague-Dawley rats. *J. Proteome Res.* **2007**, *6* (6), 2080–2093.
- (7) Karakach, T. K.; Huenupi, E. C.; Soo, E. C.; Walter, J. A.; Afonso, L. O. B.  $^1\text{H}$ -NMR and mass spectrometric characterization of the metabolic response of juvenile Atlantic salmon (*Salmo salar*) to long-term handling stress. *Metabolomics* **2009**, *5* (1), 123–137.
- (8) Charlton, A. J.; Jones, S.; Heasman, L.; Davis, A. M.; Dennis, M. Scrapie infection alters the distribution of plasma metabolites in diseased Cheviot sheep indicating a change in energy metabolism. *Res. Vet. Sci.* **2006**, *80* (3), 275–280.
- (9) He, Q. H.; Kong, X. F.; Wu, G. Y.; Ren, P. P.; Tang, H. R.; Hao, F. H.; Huang, R. L.; Li, T. J.; Tan, B.; Li, P.; Tang, Z. R.; Yin, Y. L.; Wu, Y. N. Metabolomic analysis of the response of growing pigs to dietary L-arginine supplementation. *Amino Acids* **2009**, *37* (1), 199–208.
- (10) Bertram, H. C.; Kristensen, N. B.; Malmendal, A.; Nielsen, N. C.; Bro, R.; Andersen, H. J.; Harmon, D. L. A metabolomic investigation of splanchnic metabolism using  $^1\text{H}$  NMR spectroscopy of bovine blood plasma. *Anal. Chim. Acta* **2005**, *536* (1–2), 1–6.
- (11) Pears, M. R.; Salek, R. M.; Palmer, D. N.; Kay, G. W.; Mortshire-Smith, R. J.; Griffin, J. L. Metabolomic investigation of CLN6 neuronal ceroid lipofuscinosis in affected South Hampshire sheep. *J. Neurosci. Res.* **2007**, *85* (15), 3494–3504.
- (12) Rijk, J. C. W.; Lommen, A.; Essers, M. L.; Groot, M. J.; Van Hende, J. M.; Doeswijk, T. G.; Nielen, M. W. F. Metabolomics approach to anabolic steroid urine profiling of bovines treated with prohormones. *Anal. Chem.* **2009**, *81* (16), 6879–6888.
- (13) Dumas, M. E.; Canlet, C.; Vercauteren, J.; Andre, F.; Paris, A. Homeostatic signature of anabolic steroids in cattle using  $^1\text{H}$ - $^{13}\text{C}$  HMBC NMR metabonomics. *J. Proteome Res.* **2005**, *4* (5), 1493–1502.
- (14) Wang, X. Y.; Zhao, T.; Qiu, Y. P.; Su, M. M.; Jiang, T.; Zhou, M. M.; Zhao, A. H.; Jia, W. Metabonomics approach to understanding acute and chronic stress in rat models. *J. Proteome Res.* **2009**, *8* (5), 2511–2518.
- (15) Rezzi, S.; Martin, F. P.; Alonso, C.; Guilarte, M.; Vicario, M.; Ramos, L.; Martinez, C.; Lobo, B.; Saperas, E.; Malagelada, J. R.; Santos, J.; Kochhar, S. Metabotyping of biofluids reveals stress-based differences in gut permeability in healthy individuals. *J. Proteome Res.* **2009**, *8* (10), 4799–4809.
- (16) Chen, M.; Wang, Y. Q.; Zhao, Y.; Wang, L. Q.; Gong, J. B.; Wu, L.; Gao, X. J.; Yang, Z. H.; Qian, L. J. Dynamic proteomic and metabolomic analysis reveal dysfunction and subclinical injury in rat liver during restraint stress. *Biochim. Biophys. Acta, Proteins Proteomics* **2009**, *1794* (12), 1751–1765.
- (17) Bales, J. R.; Bell, J. D.; Nicholson, J. K.; Sadler, P. J.  $\text{H-1}$ -NMR studies of urine during fasting-excretion of ketone-bodies and acetyl-carnitine. *Magn. Reson. Med.* **1986**, *3* (6), 849–856.
- (18) Connor, S. C.; Wu, W.; Sweatman, B. C.; Manini, J.; Haselden, J. N.; Crowther, D. J.; Waterfield, C. J. Effects of feeding and body weight loss on the  $\text{H-1}$ -NMR-based urine metabolic profiles of male Wistar Han rats: implications for biomarker discovery. *Biomarkers* **2004**, *9* (2), 156–179.
- (19) Horton, G. M. J.; Baldwin, J. A.; Emanuele, S. M.; Wohlt, J. E.; McDowell, L. R. Performance and blood chemistry in lambs following fasting and transport. *Anim. Sci.* **1996**, *62*, 49–56.
- (20) Kent, J. E. Stress in transported sheep. *Comp. Haematol. Int.* **1997**, *7* (3), 163–166.
- (21) Hogan, J. P.; Petherick, J. C.; Phillips, C. J. C. The physiological and metabolic impacts on sheep and cattle of feed and water deprivation before and during transport. *Nutr. Res. Rev.* **2007**, *20* (1), 17–28.
- (22) Fisher, A. D.; Niemeyer, D. O.; Lea, J. M.; Lee, C.; Paull, D. R.; Reed, M. T.; Ferguson, D. M. The effects of 12, 30, or 48 h of road transport on the physiological and behavioral responses of sheep. *J. Anim. Sci.* **2010**, *88* (6), 2144–2152.
- (23) Fan, T. W. M. Metabolite profiling by one- and two-dimensional NMR analysis of complex mixtures. *Prog. Nucl. Magn. Reson. Spectrosc.* **1996**, *28*, 161–219.
- (24) Nicholson, J. K.; Foxall, P. J. D. 750 MHz  $^1\text{H}$  and  $^1\text{H}$ - $^{13}\text{C}$  NMR spectroscopy of human blood plasma. *Anal. Chem.* **1995**, *67* (S), 793–811.
- (25) Rance, M.; Sorensen, O. W.; Bodenhausen, G.; Wagner, G.; Ernst, R. R.; Wuthrich, K. Improved spectral resolution in COSY  $^1\text{H}$  NMR spectra of proteins via double quantum filtering. *Biochim. Biophys. Res. Commun.* **1983**, *117* (2), 479–485.
- (26) Braunschweiler, L.; Ernst, R. R. Coherence transfer by isotropic mixing: Application to proton correlation spectroscopy. *J. Magn. Reson.* **1983**, *53* (3), 521–528.
- (27) Palmer, A. G.; Cavanagh, J.; Wright, P. E.; Rance, M. Sensitivity improvement in proton-detected two-dimensional heteronuclear correlation NMR spectroscopy. *J. Magn. Reson.* **1991**, *93* (1), 151–170.
- (28) Schleicher, J.; Schwendiger, M.; Sattler, M.; Schmidt, P.; Schedletzky, O.; Glaser, S. J.; Sorensen, O. W.; Griesinger, C. A general enhancement scheme in heteronuclear multidimensional NMR employing pulsed field gradients. *J. Biomol. Nmr* **1994**, *4* (2), 301–306.
- (29) Bax, A.; Summers, M. F. Proton and carbon-13 assignments from sensitivity-enhanced detection of heteronuclear multiple-bond connectivity by 2D multiple quantum NMR. *J. Am. Chem. Soc.* **1986**, *108* (8), 2093–2094.
- (30) Marion, D.; Wuthrich, K. Application of phase sensitive two-dimensional correlated spectroscopy (COSY) for measurements of  $^1\text{H}$ - $^1\text{H}$  spin-spin coupling constants in proteins. *Biochim. Biophys. Res. Commun.* **1983**, *113* (3), 967–974.
- (31) Bax, A.; Davis, D. G. MLEV-17-based two-dimensional homonuclear magnetization transfer spectroscopy. *J. Magn. Reson.* **1985**, *65* (2), 355–360.
- (32) Dieterle, F.; Ross, A.; Schlotterbeck, G.; Senn, H. Probabilistic quotient normalization as robust method to account for dilution of complex biological mixtures. Application in  $^1\text{H}$  NMR Metabonomics. *Anal. Chem.* **2006**, *78* (13), 4281–4290.
- (33) Eriksson, L., J. E., Kettaneh-Wold, N., Trygg, J., Wikstrom, C., Wold, S. *Multi- and megavariate data analysis*, Second revised and enlarged ed.; Umetrics AB: Umea, 2006.
- (34) Chilliard, Y.; Bocquier, F.; Doreau, M. Digestive and metabolic adaptations of ruminants to undernutrition, and consequences on reproduction. *Reprod. Nutr. Dev.* **1998**, *38* (2), 131–152.
- (35) Broom, D. M. Transport stress in cattle and sheep with details of physiological, ethological and other indicators. *Dtsch. Tierärztl. Wochenschr.* **2003**, *110* (3), 83–89.
- (36) Heitmann, R. N.; Sensemig, S. C.; Reynolds, C. K.; Fernandez, J. M.; Dawes, D. J. Changes in energy metabolite and regulatory hormone concentrations and net fluxes across splanchnic and peripheral-tissues in fed and progressively fasted ewes. *J. Nutr.* **1986**, *116* (12), 2516–2524.
- (37) Kanehisa, M.; Goto, S.; Furumichi, M.; Tanabe, M.; Hirakawa, M. KEGG for representation and analysis of molecular networks involving diseases and drugs. *Nucleic Acids Res.* **2010**, *38*, D355–D360.
- (38) Hoppel, C. L.; Genuth, S. M. Urinary-excretion of acetyl-carnitine during human diabetic and fasting ketosis. *Am. J. Physiol.* **1982**, *243* (2), E168–E172.
- (39) Rognstad, R. Fute cycling in carbohydrate metabolism 0.1. Background and current controversies on pyruvate cycling. *Biochem. Arch.* **1996**, *12* (2), 71–83.
- (40) Reddy, J. K.; Hashimoto, T. Peroxisomal beta-oxidation and peroxisome proliferator-activated receptor alpha: An adaptive metabolic system. *Annu. Rev. Nutr.* **2001**, *21*, 193–230.
- (41) Aramaki, S.; Lehotay, D.; Sweetman, L.; Nyhan, W. L.; Winter, S. C.; Middleton, B. Urinary excretion of 2-Methylacetacetate, 2-Methyl-3-hydroxybutyrate and Tiglylglycine after Isoleucine loading in the

- diagnosis of 2-Methylacetoacetyl-CoA thiolase deficiency. *J. Inherited Metab. Dis.* **1991**, *14* (1), 63–74.
- (42) Bonafe, L.; Troxler, H.; Kuster, T.; Heizmann, C. W.; Chamois, N. A.; Burlina, A. B.; Blau, N. Evaluation of urinary acylglycines by electrospray tandem mass spectrometry in mitochondrial energy metabolism defects and organic acidurias. *Mol. Genet. Metab.* **2000**, *69* (4), 302–311.
- (43) Dosman, J.; Crawhall, J. C.; Klassen, G. A.; Mamer, O. A.; Neumann, P. Urinary excretion of C6–C10 dicarboxylic acids in glycogen storage disease types I and III. *Clin. Chim. Acta* **1974**, *51* (1), 93–101.
- (44) Mortensen, P. B.; Gregersen, N. The biological origin of ketotic dicarboxylic aciduria 2. In vivo and in vitro investigations of the beta-oxidation of C8-C16-dicarboxylic acids in unstarved, starved and diabetic rats. *Biochim. Biophys. Acta* **1982**, *710* (3), 477–484.
- (45) Vickers, A. E. M. Characterization of hepatic mitochondrial injury induced by fatty acid oxidation inhibitors. *Toxicol. Pathol.* **2009**, *37* (1), 78–88.
- (46) O'Donoghue, N.; Sweeney, T.; Donagh, R.; Clarke, K. J.; Porter, R. K. Control of choline oxidation in rat kidney mitochondria. *Biochim. Biophys. Acta-Bioenerg.* **2009**, *1787* (9), 1135–1139.
- (47) Burg, M. B.; Ferraris, J. D.; Dmitrieva, N. I. Cellular response to hyperosmotic stresses. *Physiol. Rev.* **2007**, *87* (4), 1441–1474.
- (48) Robinson, B. S.; Snoswell, A. M.; Runciman, W. B.; Kuchel, T. R. Choline biosynthesis in sheep-evidence for extrahepatic synthesis. *Biochem. J.* **1987**, *244* (2), 367–373.
- (49) Martin, A. K. The origin of urinary aromatic compounds excreted by ruminants. 1. The metabolism of quinic, cyclohexanecarboxylic and non-phenolic aromatic acids to benzoic acid. *Br. J. Nutr.* **1982**, *47* (1), 139–154.
- (50) Martin, A. K. The origin of urinary aromatic compounds excreted by ruminants. 2. The metabolism of phenolic cinnamic acids to benzoic acid. *Br. J. Nutr.* **1982**, *47* (1), 155–164.
- (51) Williams, R. E.; Eyton-Jones, H. W.; Farnworth, M. J.; Gallagher, R.; Provan, W. M. Effect of intestinal microflora on the urinary metabolic profile of rats: a H-1-nuclear magnetic resonance spectroscopy study. *Xenobiotica* **2002**, *32* (9), 783–794.
- (52) Curtius, H. C.; Mettler, M.; Ettlinger, L. Study of the intestinal tyrosine metabolism using stable isotopes and gas chromatography-mass spectrometry. *J. Chromatogr.* **1976**, *126* (NOV3), 569–580.
- (53) Martin, A. K. Urinary aromatic acid excretion by fed and fasted sheep in relation to protein metabolism in the rumen. *Br. J. Nutr.* **1973**, *30* (2), 251–267.
- (54) Kawakami, K.; Kojima, K.; Makino, I.; Kato, I.; Onoue, M. Fasting enhances p-Cresol production in the rat intestinal tract. *Exp. Anim.* **2007**, *56* (4), 301–307.
- (55) Yap, I. K. S.; Li, J. V.; Saric, J.; Martin, F. P.; Davies, H.; Wang, Y. L.; Wilson, I. D.; Nicholson, J. K.; Utzinger, J.; Marchesi, J. R.; Holmes, E. Metabonomic and microbiological analysis of the dynamic effect of vancomycin-induced gut microbiota modification in the mouse. *J. Proteome Res.* **2008**, *7* (9), 3718–3728.
- (56) Bertini, I.; Calalbro, A.; De Carli, V.; Luchinat, C.; Nepi, S.; Porfirio, B.; Renzi, D.; Saccenti, E.; Tenori, L. The metabonomic signature of celiac disease. *J. Proteome Res.* **2009**, *8* (1), 170–177.
- (57) Wang, Y. L.; Xiao, S. H.; Xue, J.; Singer, B. H.; Utzinger, J.; Holmes, E. Systems metabolic effects of a *Necator americanus* Infection in Syrian Hamster. *J. Proteome Res.* **2009**, *8* (12), 5442–5450.
- (58) Wikoff, W. R.; Anfora, A. T.; Liu, J.; Schultz, P. G.; Lesley, S. A.; Peters, E. C.; Siuzdak, G. Metabolomics analysis reveals large effects of gut microflora on mammalian blood metabolites. *Proc. Natl. Acad. Sci. U.S.A.* **2009**, *106* (10), 3698–3703.
- (59) Williams, H. R. T.; Cox, I. J.; Walker, D. G.; North, B. V.; Patel, V. M.; Marshall, S. E.; Jewell, D. P.; Ghosh, S.; Thomas, H. J. W.; Teare, J. P.; Jakobovits, S.; Zeki, S.; Welsh, K. I.; Taylor-Robinson, S. D.; Orchard, T. R. Characterization of inflammatory bowel disease with urinary metabolic profiling. *Am. J. Gastroenterol.* **2009**, *104* (6), 1435–1444.
- (60) Blaxter, K. L.; Graham, N. M. Plane of nutrition and starch equivalents. *J. Agr. Sci.* **1955**, *46* (03), 292–306.
- (61) Kim, G. S.; Chevli, K. D.; Fitch, C. D. Fasting modulates creatine entry into skeletal-muscle in the mouse. *Experientia* **1983**, *39* (12), 1360–1362.
- (62) Adibi, S. A. Metabolism of branched-chain amino-acids in altered nutrition. *Metab., Clin. Exp.* **1976**, *25* (11), 1287–1302.
- (63) Marchesini, G.; Bianchi, G. P.; Vilstrup, H.; Capelli, M.; Zoli, M.; Pisi, E. Elimination of infused branched-chain amino-acids from plasma of patients with nonobese type-2 diabetes-mellitus. *Clin. Nutr.* **1991**, *10* (2), 105–113.
- (64) Vazquez, J. A.; Paul, H. S.; Adibi, S. A. Regulation of leucine catabolism by caloric sources-role of glucose and lipid in nitrogen sparing during nitrogen deprivation. *J. Clin. Invest.* **1988**, *82* (5), 1606–1613.
- (65) Veerkamp, J. H.; Vanmoerkerk, H. T. B.; Wagenmakers, A. J. M. Interaction of short-chain and branched-chain fatty-acids and their carnitine and CoA esters and of various metabolites and agents with branched-chain 2-oxo acid oxidation in rat muscle and liver-mitochondria. *Int. J. Biochem.* **1985**, *17* (9), 967–974.
- (66) Thompson, J. R.; Wu, G. The effect of ketone bodies on nitrogen metabolism in skeletal muscle. *Comp. Biochem. Physiol., Part B: Biochem. Mol. Biol.* **1991**, *100* (2), 209–216.
- (67) Chung, Y.-L.; Wassif, W. S.; Bell, J. D.; Hurley, M.; Scott, D. L. Urinary levels of creatine and other metabolites in the assessment of polymyositis and dermatomyositis. *Rheumatology* **2003**, *42*, 298–303.
- (68) Connor, S. C.; Gray, R. A.; Hodson, M. P.; Clayton, N. M.; Haselden, J. N.; Chessell, I. P.; Bountra, C. An NMR-based metabolic profiling study of inflammatory pain using the rat FCA model. *Metabolomics* **2007**, *3* (1), 29–39.
- (69) Poirier, Y.; Antonenkov, V. D.; Glumoff, T.; Hiltunen, J. K. Peroxisomal beta-oxidation - A metabolic pathway with multiple functions. *Biochim. Biophys. Acta: Mol. Cell Res.* **2006**, *1763* (12), 1413–1426.
- (70) Hunt, M. C.; Alexson, S. E. H. Novel functions of acyl-CoA thioesterases and acyltransferases as auxiliary enzymes in peroxisomal lipid metabolism. *Prog. Lipid Res.* **2008**, *47* (6), 405–421.
- (71) Schrader, M.; Yoon, Y. Mitochondria and peroxisomes: are the 'Big Brother' and the 'Little Sister' closer than assumed? *Bioessays* **2007**, *29*, 1105–1114.
- (72) Veerkamp, J. H.; Van Moerkerk, H. T. B. Peroxisomal fatty acid oxidation in rat and human tissues, Effect of nutritional state, clofibrate treatment and postnatal development. *Biochim. Biophys. Acta* **1986**, *875* (2), 301–310.
- (73) Piot, C.; Veerkamp, J. H.; Bauchart, D.; Hocquette, J.-F. Contribution of mitochondria and peroxisomes to palmitate oxidation in rat and bovine tissues. *Comp. Biochem. Physiol., Part B: Biochem. Mol. Biol.* **1998**, *121* (2), 185–194.